A THESIS

On

Studies on some glass sealants for solid oxide fuel cells

Submitted in the partial fulfillment of requirement for the award of the degree of

Master of Technology (M. Tech)

IN

MATERIALS SCIENCE AND ENGINEERING

Submitted by
VISHAL KUMAR
Roll No. : 6040507

Under the guidance of

Dr Kulvir Singh
Assistant Professor

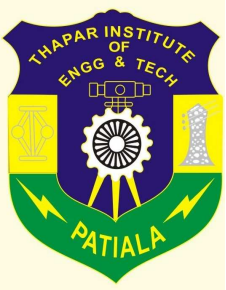

School of Physics and Materials Science

THAPAR INSTITUTE OF ENGINEERING AND TECHNOLOGY

(DEEMED UNIVERSITY)

PATIALA (PUNJAB)-147004

JULY 2006

CERTIFICATE

This is to certify that the thesis entitled **STUDIES ON SOME GLASS SEALANTS FOR SOLID OXIDE FUEL CELLS** submitted by **Mr. Vishal Kumar** in the partial fulfillment of the requirement for the award of the degree of **M. Tech** in **Materials Science and Engineering** from the **School of Physics and Materials Science, Thapar Institute of Engineering and Technology (Deemed University), Patiala,** is a record of candidate's own work carried out by him under my supervision and guidance. The matter embodied in this report has not been submitted in part or full to any other university or institute for the award of any degree.

(Dr. Kulvir Singh)

Assistant Professor & P.G Incharge

School of Physics and Materials Science

Thapar Institute of Engg. & Technology, Patiala, Punjab (147004)

Countersigned by:

(Dr. O.P. Pandey)

Professor and Head, SPMS

Thapar Institute of Engg. & Technology,

Patiala, Punjab (147004)

(Dr. T.P. Singh)

Dean, Academic Affairs

Thapar Institute of Engg. & Technology,

Patiala, Punjab (147004)

Dated:

ACKNOWLEDGEMENTS

I express my deep gratitude and respects to my guide **Dr. Kulvir Singh for** his keen interest and valuable guidance, strong motivation and constant encouragement during the course of the work. I thank him from the depths of my heart for introducing me to the area of solid oxide fuel cells. I thank him for his great patience, constructive criticism and myriad useful suggestions apart from invaluable guidance to me.

I am grateful to **Dr. O.P. Pandey, Professor and Head, School of Physics and Materials Science** for his encouragement and execution of thesis work.

No task is single man's effort .Various factors, situations and persons integrate to provide the background for the accomplishment of a task. Foremost, I'm indebted to God almighty that has been there today and always.

My project would not have seen daylight without the immense cooperation of my friends **Ashutosh Goel** and **Anu Arora** who helped me at various stages during the due course of my work.

My sincere thanks to **Mr. Purushotam.** MSD, T.C.I.R.D, Patiala for his help to carry out X-Ray diffraction studies.

The help provided by **Dr. Piyush Verma, Sh. Daljit Singh, S. Jant Singh** is highly acknowledged**.**

I am greatful to my friends **Mohit, Himani, Komal, Deepti** & **Sameer** for their cooperation and support.

I owe my sincere thanks to all the staff members of **School of Physics and Materials Science** for their support and encouragement.

Last but not the least; I would like to thank **my parents** for their moral support that kept my spirit up during the endeavor.

Vishal Kumar

ABSTRACT

Planar design of Solid Oxide Fuel Cell (SOFC) is better than tubular design due to its higher current density and simple manufacturing. However, the planar design of SOFC requires sealants at the edges of the cells to prevent fuel leakage and air mixing at higher temperature. The glass and glass ceramics are most suitable and compatible with other components of SOFC at working temperature of SOFC (800-1000^{o}C). In the present study a series of SiO_2-B_2O_3-MgO/SrO-A_2O_3 (A= Y, La, Al) compositions have been synthesized by taking appropriate proportion (mol %) of each oxide constituents. The as cast samples were characterized by using various techniques viz X-Ray diffraction (XRD), Dilatomterey, Fourier Transform Infrared Spectroscopy (FTIR) and differential thermal analysis (DTA).Amorphous nature of all the as cast samples is confirmed by x-ray diffraction. Absorption bands of all glass samples are composed of silicate and borate chains. The dilatomterey and DTA analysis were done to find the thermal expansion coefficient (TEC) and stability respectively. In order to understand the crystallization kinetics these samples were heat treated at 800^{o}C for various heat treatment durations. A detailed structural thermal and bonding nature of glasses has been presented in this report.

CONTENTS

CHAPTER-1

INTRODUCTION

1.1 Background:

Over the past several decades there have been a lot of efforts to develop alternative methods of power generation so as to meet the ever increasing demand of the rising population. Among all other candidates, Fuel cells are very important. Fuel cell converts the chemical energy of fuels directly into electricity .The principle of the fuel cell developed by William Grove in 1939[1]. At that time a large number of scientists and engineers were predicting that fuel cell would be efficient and clean source of energy. Still a lot of development is required for this technology to be successful and commercialized.

Apart from fuel cells scientists and engineers have knowledge of many other energy conversion technologies but the focus is on fuel cells because of efficiency and technology that is eco-friendly

With advancement in processing techniques, development of fuel cell technology is getting attention in all over the world so that this clean source of energy can be commercialized.

1.2 Working of Fuel Cell:

The primary function of any fuel cell of a fuel cell is to produce an electrical current via electrochemical reaction .Because there is no intermediate thermal conversion step and therefore no attendant carnot cycle limitation. These devices provide highly efficient means of electrical power generation.

There are several kinds of fuel cells, and each operates a bit differently. But, in general terms, hydrogen atoms enter a fuel cell at the anode where a chemical reaction (with hydrogen) strips them of their electrons. The hydrogen atoms are now “ionized,” and carry a positive electrical charge. The negatively charged electrons provide the current outer circuit. If alternating current (AC) is needed, the DC output of the fuel cell must be passed through a conversion device called an inverter.

Oxygen enters the fuel cell at the cathode side and, in some cell types (like the one illustrated above), oxygen atoms combines with electrons (returning from the electrical circuit) and hydrogen ions that have traveled through the electrolyte from the anode.

In other words the overall reaction takes place in cathode side. In other cell types the oxygen picks up electrons and then travels through the electrolyte to the anode, where it combines with hydrogen ions. Whether reaction is taking place at anode or cathode side, in both the cases hydrogen and oxygen form water. As long as a fuel cell is supplied it can generate electricity.

The electrolyte plays an important role in fuel cell. It must permit only the appropriate ions to pass between the anode and cathode. If free electrons or other substances could travel through the electrolyte, they would disrupt the chemical reaction.

Fuel cells are electrochemical devices like batteries that convert the chemical energy, of a reaction directly into electric energy. However, unlike batteries, which function as storage devices and therefore stop providing energy as soon as the reactants are used up, fuel cells operate continuously as long as fuel (hydrogen) is supplied.

A typical working of fuel cell is given in figure.1

$$\text{Anode: } H_2 + O^{2-} \longrightarrow H_2O + 2e^-$$

$$\text{Cathode: } 1/2\ O_2 + 2e^- \longrightarrow O^{2-}$$

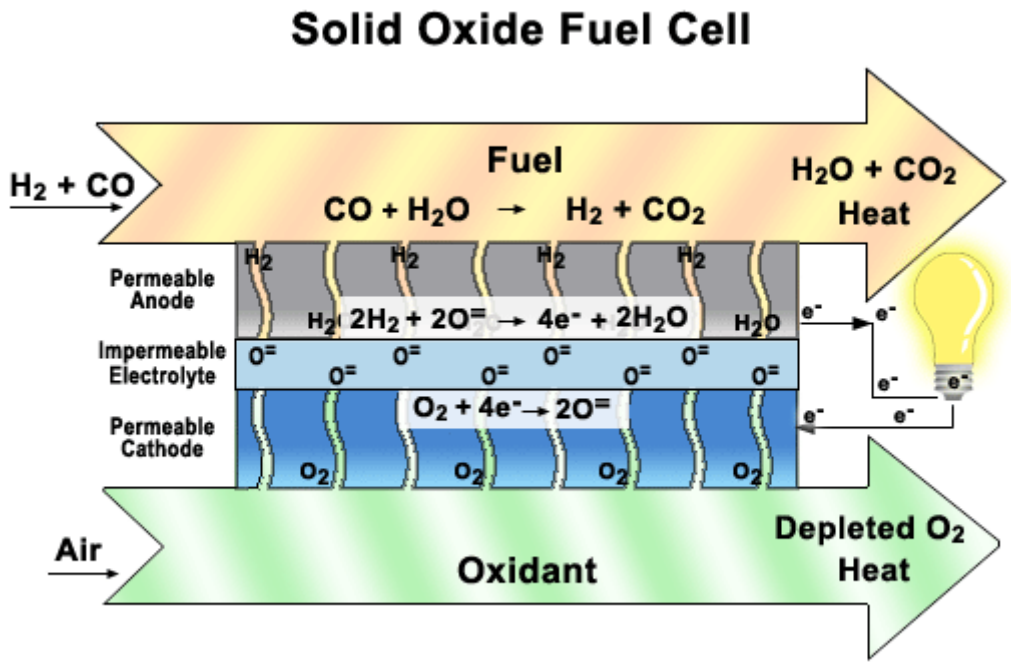

Fig. 1 Fuel cell

Based on their electrolytes fuel cells can be categorized as follows.

1. Alkaline fuel cell (AFC)

2 .Molten carbonate fuel cell (MCFC)

3 .Solid oxide fuel cell (SOFC)

Among the fuel cells, solid oxide fuel cell has some advantage over the other cells such as it can be made of relatively cheap ceramic material along with the provision of different varieties of fuels such as H_2, CH_4 etc can be used

Based on the stacking, SOFC can be categorized in two categories namely, planar and tubular design. Planar type has received growing attention in comparison to the tubular because of its simple manufacturing, relatively high current density and higher efficiency.

However, planar design must overcome an important challenge which does not apply to tubular system. In case of planar SOFC design, one of the most critical materials is the gas seal that must be applied along the edges of each cell and between the stack and gas manifolds. Glass and glass ceramics meet most of the requirements required for sealing at high temperature. Formation, properties and other details of glass and glass sealants, which are required for sealing in planar design of SOFC, will be presented in next chapters.

CHAPTER 2

GLASS SEALANTS IN SOFC

DESIGN

2.1 Glass Sealants in SOFC Design:

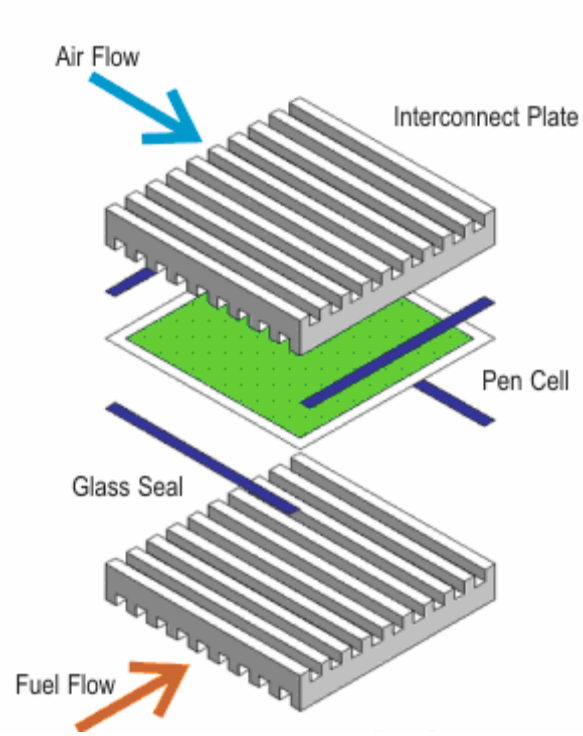

Fig. 2.1 Exploded view of stacked SOFC

Within the SOFC it is important that the fuel and air streams are kept separate, and that a thermal balance should be maintained to ensure that the temperature of operation remains within an acceptable range. Several designs of SOFC have been developed to accommodate these requirements; one option is shown schematically in Figures 2.1 and 2.2.

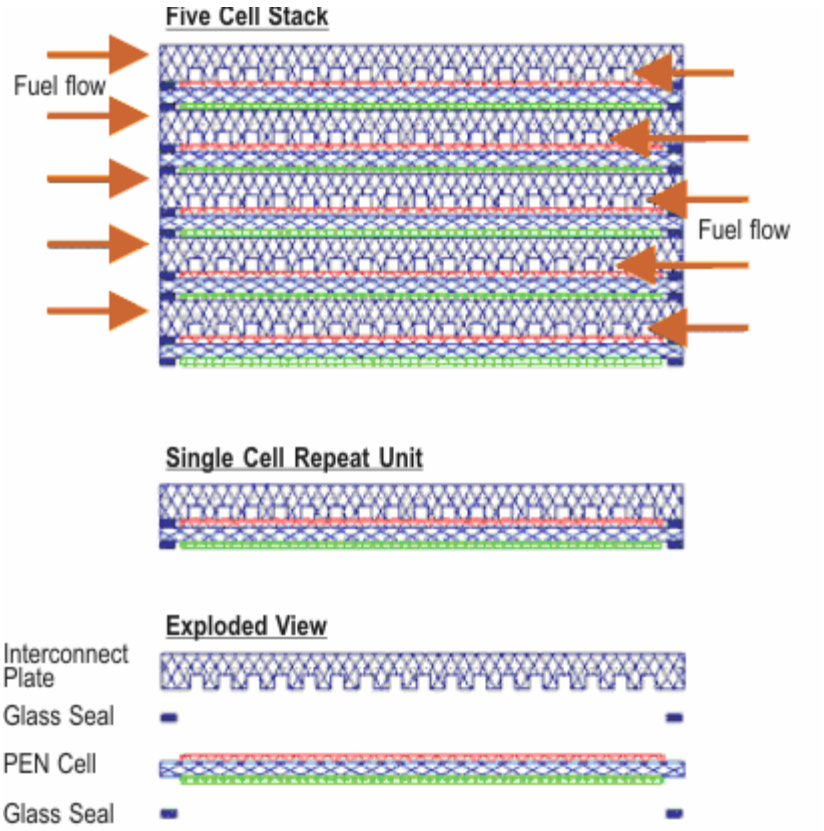

Fig. 2.2 Planar design

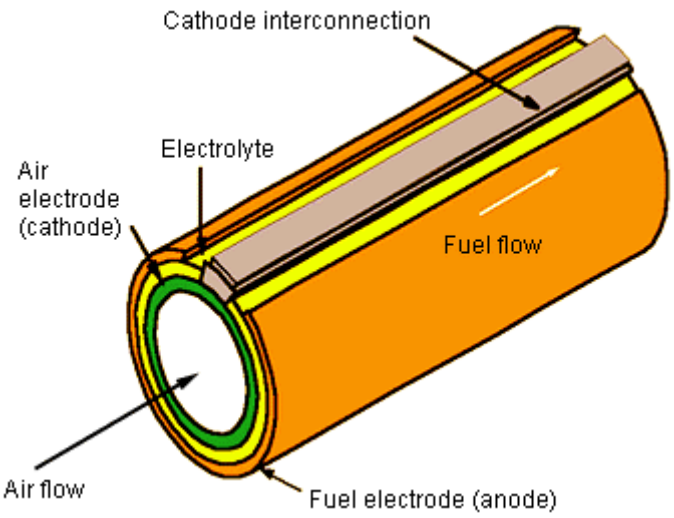

Fig. 2.3 Tubular design

The SOFC design has undergone different modifications and more are being suggested and implemented. This has brought a complete change into its stacking sequence and ultimately, a change in design of complete system. At present the stacking design and fabrication consist of four common stack configurations that have been proposed and fabricated for SOFCs: sealless tubular design, segmented-cell-in-series design, monolithic design and flat-plate design.

The designs differ in the extent of dissipative losses within the cells, in the manner of sealing between fuel and oxidant channels, and in the manner of making cell-to-cell electrical connections in a stack of cells. Articles describing various aspects of these designs had already been published [1, 8]. Out of these four designs, the flat plate (planar) and seal-less tubular [Figure 2.1 and Figure 2.3] designs have been seen with alacrity. As the name suggests, sealless tubular design has a distinct feature that it has no seals; therefore, the problems with the gastight seals for ceramics at high temperatures are eliminated. This design has an additional advantage that each single cell is built as a unit structure. This allows some freedom of thermal expansion and minimizes the problem of cracking caused by undue thermally induced stresses in a monolithic pack of connected cells. However apart from these promotional positive points, some loopholes accompany this design too, which severely hamper the performance of a fuel cell, and thus cannot be ignored. The sealless tubular design has a relatively long current path through the cell. The current path is long in the plane of the electrodes, resulting in greater resistive loss.

The support tube is a limitation on cell performance. The thick support tube restricts the amount of oxygen, which can be transported to the cathode/electrolyte interface. Thus gas diffusion through the tube can become the rate-limiting step and sets the limiting current for the cell. Even below the limiting current, gas transport represents the loss in cell performance. Comparatively on the other hand, the flat plate design offers improved performance and improved power density relative to the tubular and segmented-cell-in-series design. Certain factors such as in-plane conduction, internal resistance losses of flat-plate SOFCs are independent of cell area.

Due to this cell components can be made very thin to minimize the electrical resistance and also the fabrication of flat-plate designs is simpler .The two dense components, the electrolyte and the interconnect, can be fabricated independently. This avoids the

difficulties in co-sintering of the ceramic interconnect and provides multiple processing options. Apart from this, the fabrication of flat-plate SOFC allows cell components to be assessed individually, thus, ensuring better quality control [8]. However, the flat-plate (planar) design must overcome a significant challenge, which does not apply to tubular systems. The requirement for effective, high temperature seals to prevent fuel leakage and air mixing at high temperature along with to seal the electrolyte against the metallic body of the device, in order to create a hermetic, rugged and stable stack is the urgent requirement of the planar design [Figure 2.1].

Any leakage of fuel into the air (or air into the fuel) will lead to direct combustion of fuel and may cause local overheating (hot spots) and sometimes may burst .It is necessary to seal the electrodes properly to prevent the fuel gas and air from mixing during the operation . The cathode is required to be sealed on the fuel inlet and outlet side while the anode is to be sealed on the air inlet and outlet side.

Typical conditions under which the SOFC is expected to operate and to which the seal will be exposed include [10, 11]:

- An average operating temperature of 750^{o}C.
- Continuous exposure to an oxidizing atmosphere on the cathode side and a wet reducing gas on the anode side.
- An average oxygen partial pressure in the range from 2 x 10^{4} to 1 x 10^{-13} Pa.
- An anticipated device lifetime of more than 10,000 hours.

CHAPTER 3

SEALANTS AND THEIR PROPERTIES

3.1 Sealants:

The application to which the stack will be subjected determines the selection criteria for sealing materials/techniques. The various factors that affect the seal performance are individual cell and stack materials and geometries, stack assembly sequence, thermal gradients expected across the seal and other stack components, maximum weight and/or volume of the power plant, anticipated external forces, and required heating and/or cooling rate of the device. Table 1 gives a detailed list of generic set of requirements for the SOFC seals [10].

Table 1 Requirements for planar SOFC seals

Mechanical • Hermetic/marginal leak rate • TEC matching • Acceptable bond strength or compressive loading requirement (i.e. load frame design) • Resistant to degradation due to thermal cycling/thermal shock • Robustness under external static and dynamic forces	**Chemical** • Long –term chemical stability under simultaneous oxidizing/wet fuel environments • Long-term chemical compatibility with the adjacent sealing surfaces • Resistance to hydrogen embrittlement
Design/fabrication • Low cost • Facile application/processing • High reliability with respect to achieving initial hermeticity (i.e. seal conforms to non-flat substrate surfaces) • Design flexibility	**Electrical** • Non-conductive (non-shorting configuration)

3.2 Methods of Sealing:

For the joining of ceramics to other ceramics or to metals many different techniques are available. Depending upon types of joining processes there are three general categories. In the first, attachment is mechanical and is achieved through the use of mechanical interlocking of components.

Provided that the materials are refractory and chemically compatible, this approach should provide high strength at high temperatures. However, it has been pointed out that the lack of ductility in ceramics severely limits the temperature range over which the method is applicable because of the high local tensile stresses that can develop in systems with thermal expansion mismatches, causing failure in the ceramics [12]. Moreover, it has been observed that successful application of mechanical attachment in demanding environments is difficult to achieve, especially if leak tight joints are required or if the joint will be subjected to thermal cycling [13]. The second approach is direct joining, in which components are bonded either by solid – state process or by fusion.

Direct joining or solid-state pressure bonding has been applied to joining of ceramics to ceramics and ceramics to metals [14-17]. Successful pressure bonding relies upon the achievement of adequate interfacial contact and subsequent diffusion or plastic flow to eliminate interfacial porosity.

The advantages of solid-state pressure bonding include a simple fabrication procedure, a one-step process, and potentially very high joint strength. However, this method is not free from certain limitations and disadvantages which include: high cost; only flat specimens can be joined; a vacuum/inert atmosphere is required; and a pressure must be applied. The need for pressure application during diffusion bonding imposes restrictions on the joint geometry; most joints are of face seal type and are not well suited for accommodating thermal expansion mismatch. As a result, the bonded components must either be small, one component must be thin or the TEC of the components must be well matched. The third approach could be referred to as indirect joining in the sense that an intermediate layer of material, such as an adhesive, cement, or braze is used to bond two components. The use of a liquid, a glass, or a solid foil readily under low applied stress to join materials can prove to be advantageous. Flow of a wetting liquid or glass or of the ductile solid can fill irregularities in the surface and therefore impose less stringent

demands on surface preparation and degree or extent of surface mating required. Ductile metal interlayer can undergo plastic flow and thus reduce the stress that builds up in the ceramic during thermal cycling [18-20].

Based on these three approaches, various high temperature-sealing techniques have been developed.

- Diffusion bonding
- Reaction bonding
- Active metal brazing
- Air brazing
- Bonded compliant sealing
- Compressive sealing
- Rigid bonding or glass joining

Each of these techniques has some added inherent advantages and limitations. The salient features and drawbacks of the above mentioned sealing methods are discussed in brief with special emphasis on compressive seals and rigid bonding.

Diffusion Bonding:

Diffusion bonding is a solid-state welding process wherein coalescence of contacting surfaces is produced with minimum macroscopic deformation by diffusion-controlled processes, which are induced by applying heat and pressure for a finite interval [21]. By means of diffusion bonding, it is possible to bond all materials whose chemical and metallurgical properties are compatible. Since bonding of advanced materials using the classical welding methods [22] is not possible due to unexpected phase propagation at the bond interface [23], the diffusion bonding technique can be employed to bond such materials. This technique is dependent on a number of parameters, in particular, time, applied pressure, bonding temperature and method of heat application. Diffusion bonding usually takes place in a uniaxial press (hot Isostatic pressing can be used but requires more complex fixturing) heated via elements or induction units. This also presents a restriction on the size of components that be processed. However, a more recent

innovation uses microwave heating and this has been shown to produce excellent bonds in a matter of minutes, but still for components no bigger than a shoebox. Ceramic-ceramic diffusion bonding is difficult to achieve unless either diffusion aids or (more commonly) secondary phases are present. These are most typically glassy phases at grain boundaries. Moreover, there is usually an added complication when joining dissimilar materials - the differences in thermal expansion coefficient (TEC). This can cause strains to develop at the interface, which can cause premature failure of the bond.

The extreme conditions required for diffusion bonding generally make this technique incompatible with the planar stack fabrication.

Reaction bonding:

Reaction Bonding (RB) is a ceramic casting process. Silicon carbide grains are mixed with water and binding agents to form slurry, cast into a mold and then freeze dried to remove the water. This part is then sintered to form a porous alpha SiC structure. A high temperature process then introduces silicon into the porous structure and results in a 100% dense structure consisting of a bonded network of silicon carbide with isolated regions of free silicon (10-30%). The reaction bonding process has shrinkage of less than 0.5%. Use of a fugitive core allows substrates to be cast with integral backs.

While the reaction bonding has been used to join non-oxide ceramics like SiC, less success has been demonstrated with forming hermetic ceramic-to-metal joints. The joints formed by this technique often contain residual porosity, shrinkage-induced cracks, unconverted reactants, and undesired secondary product phases, each of which can reduce the overall joint strength [24].

Active metal brazing:

Brazing is a process in which two or more closely fitting parts are joined via an intermediate metallic material, which melts, wets the surface being joined, reacts and finally solidifies. Brazing does not involve any melting or plastic state of the base metals. The joining of an assembly of two or more metal parts into a structure is achieved by heating the assembly to a temperature high enough to melt the filler metal but not the parts. The molten filler metal spreads into the joint and must wet the base-metal surfaces.

Dissimilar metals that cannot be joined by a traditional welding process, because of their metallurgical incompatibilities or complex geometry, can be brazed successfully. Two basic mechanisms are involved in bond formation, by wetting the surfaces with the braze alloy, and consequent interface reaction with the two surface layers of some micrometer thickness. If these layers increase in thickness the bond strength of the joints may be degraded, promoting failure by interfacial stresses due to thermal expansion mismatch [25]. The technique of active metal brazing utilizes filler metal that when heated above its liquidus temperature will flow and fill the gap between the two joining pieces by capillary action. Unlike metal-to-metal brazes, this particular family of braze alloys contains one or more reactive metals, often titanium, which will chemically reduce the ceramic at the interface with the braze, greatly improving wetting and adherence between the two materials [26, 27].

However, two problems are encountered when using this technique to solid-state electrochemical devices:

- The joint is not sufficiently resistant to oxidation, and will degrade under high-temperature operation [28].
- Joining must be conducted in a high-temperature, reducing gas environment, a condition that is too demanding for many of the p_{O2} –sensitive oxides used in the fuel cell [29].

Air brazing:

This is a new concept under investigation at Pacific Northwest National Laboratory (PNNL), USA [30]. It is a method of ceramic-to-metal brazing specifically for fabricating high-temperature solid-state devices such as oxygen generators in which braze pastes are formulated by mixing appropriate ratio of copper and silver powders with a standard screen printing binder. Disc-shaped bilayer coupons of requisite dimensions are fabricated by traditional tape casting and co-sintering techniques and are tested on SOFC components.

This technique differs from the metal brazing in two important ways [10]:

- It uses a liquid-phase oxide/noble metal melt as the basis for joining, and therefore exhibits high-temperature oxidation resistance.
- The process is conducted directly in air without the use of fluxes and/or inert cover gases.

Bonded Compliant Seal:

This is another sealing concept being tried at PNNL, which can employ a number of high temperature alloys for use as the foil membranes. Experiments are being conducted using commercial alumina-forming ferritic steel as the foil membrane: DuraFoil (22% Cr, 7% Al, 0.1% La+Ce, balance Fe, manufactured by Engineered Materials Solutions Inc, Attleboro, MA) [10].

However, the research on the concept of air brazing and bonded compliant seals is at initial stages and their long-term durability, as well as the potential for scale up and prototype use in demonstration stacks is still to be proved.

Compressive Sealing:

Compressive seals utilize materials such as sheet structure silicates, which do not bond to the SOFC components; instead the sealing material acts as a gasket and the seal is achieved by applying a compressive force to the stack. In comparison to the rigid seals (discussed in the next section), compressive seals potentially offer several advantages. Since, they are not rigidly bonded to the cells; the need for matching thermal expansion coefficient (TEC) of all the stack components is reduced or eliminated. The cells and the interconnects are allowed to expand and contract freely during thermal cycling and routine operation. Elimination of the need of matching TEC greatly expands the list of candidate interconnect materials, whether ceramic or metallic [31]. However, the use of compressive seals bring new challenges to the SOFC stack design- a load frame must be included to maintain a desired level of compressive load during operation, and the stack components must be able to withstand the compressive load required for adequate sealing for the lifetime of the stack [32]. The commercial derivatives of mica (class = phyllosilicates; general formula = $AB_{2-3}(X,Si)_4O_{10}(O,F,OH)_2$) like muscovite

($KAl_2(AlSi_3O_{10})(F,OH)_2$), phlogopite ($KMg_3(AlSi_3O_{10})(OH)_2$) are being considered as a potential base material in compressive seals [33-37]. Researchers at PNNL, [31, 32, 34-37] and Forschungszentrum Jülich, Germany [38] are actively engaged in assessing the potential of mica as a compressive seal for intermediate temperature (~800^oC) SOFC. Fig. 11 shows the various types of mica seals.

Simner and Stevenson [35] examined micas in paper form as well as the cleaved single crystal form. The results showed the cleaved natural mica sheets to be far superior compared to mica papers, however, the coupon leak rate shown by the latter was also not acceptable for actual SOFC stacks, in which, multiple, full size components would be stacked together with the mica gaskets between each component. The problem of reducing the leak rates as admissible to the actual stack conditions led to the birth of a novel hybrid mica-based seal in which the leak rate can be reduced ~4300 times by simply adding the glass interlayer between the mica and the adjacent stack components

For an ideal hermetic seal, the leak rate should be zero. Practically, the actual low leak rates were limited by the system's background. Low fuel leak rate are required if SOFC stacks are to operate safely and economically. Although, the allowable leak rate remain to be determined and will be somewhat offering leak rates as low as possible at compressive stress as low as possible. The hybrid seal based on muscovite single crystal mica appears to be a viable candidate [40].

The use of compressive seals brings several new challenges to SOFC stack design- a load frame must be included to maintain the desired level of compressive load during operation, and the stack components must be able to withstand the compressive load required for adequate sealing for the lifetime of the stack. The problems have been found with the natural variance in thickness of mica sheets and relative non-compressibility of the mica. Also, it has been found that mica may leach minerals into the cell and poison the catalyst [41]. These factors prevent an effective seal from forming. At present, however, this technology remains incomplete due to the lack of reliable high temperature sealing material that would form the basis of the compressive seal.

Rigid bonding or glass joining:

A number of materials have been considered for compressive sealing, including, mica, nickel and copper, but each has been found deficient for several reasons, including the oxidation resistance in the case of metals to poor hermiticity and also the seal leakage in the case of mica [33]. Material oxidation and load relaxation due to creep, as well as added expense and additional thermal mass that must be heated, cooled and maintained at temperature under the equilibrium operation are all issues that require particular attention with this type of cell design. Due to these constraints and specifically because our application is an auxiliary power unit (APU) where minimization of device weight and volume are critical, rigid seals are good choice such as glass sealants [42]. The majority of SOFC seal development has focused on bonded, rigid seals; primarily glass and glass-ceramics, which essentially "glue" the stack components together. Many glass seals are deigned to soften, and viscously flow above the SOFC operating temperature to provide hermetic seals by mechanical/chemical bonding. On cooling back down to operating temperature, the glass crystallizes to form a rigid, bonded seal. A principal advantage of glass seals is that the glass composition can be tailored to optimize some of the physical properties, such as thermal expansion coefficient (TEC).

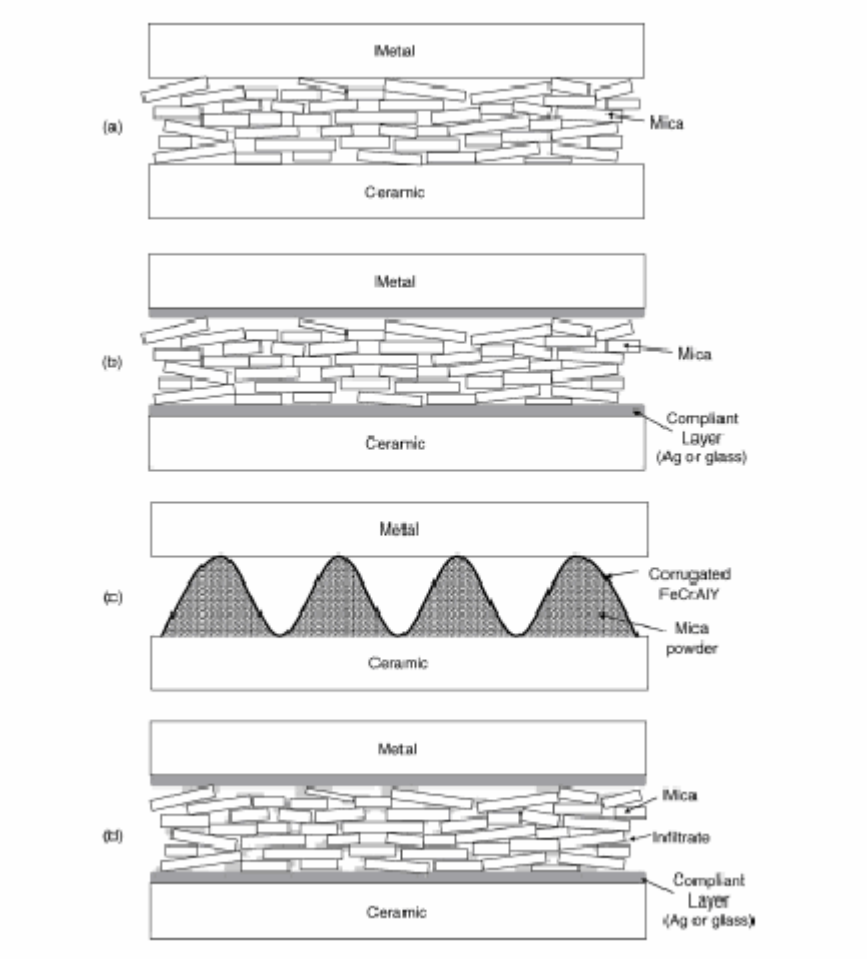

Fig. 3.1 Mica seals (a)plain mica seal [31, 39] (b)hybrid mica seal with compliant layer(glass or metal) [31,39] (c)mica powder with corrugated alloy[38] (d) hybrid mica seal with compliant layer and infiltrate mica[36].

3.3 Current Status of Glass Sealant:

A sealing material has to fulfill some critical requirements as described above, because the operation temperature of the SOFC is almost 850°C and the operation period must be more than 5 years. Other major requirements are [9]:

- No chemical reaction with the joining components and solder stability in oxidizing and wet reducing atmospheres;
- Viscosity: 10^5 Pa-s at joining temperature (1000°C) and $>10^9$ Pas at operating temperature (850°C);
- Only a small thermal expansion mismatch with respect to SOFC components (TEC=$11X10^{-6}$ K^{-1});
- Leakage rate of joining should be less than 10^{-7} mbar $1s^{-1}$ per cm joined length;
- Resistivity more than 2 KΩ cm^2.

However, several challenges remain with respect to the use of glass seals in SOFCs. The brittle nature of glasses below the glass transition temperature makes the seals vulnerable to crack formation, and glasses tend to react with other cell components, such as electrodes, at SOFC operating temperatures. Glass seals can affect electrode performance over a short range (via solid state diffusion or viscous flow) or over longer distances (via gaseous transport of glass constituents).

3.31 Problems with Glass Sealants

Potentially there are several ways in which a rigid glass seal can fail during operation, including the following:

- *Failure by fracture under pressure.* The glass seal can be viewed essentially as a multicomponent laminate composite composed of the electrolyte, the sealing glass and the oxide scale that naturally forms on the metal substrate during stack sealing and operation. Each of these layers is a brittle material and as such, each is susceptible to failure by brittle fracture. Thus, if a large enough flaw exists in any of the materials with in the seal or if the residual tensile stresses of a minimum

critical value develop due to thermal expansion mismatch between components or warping due to non-uniform heating with in a given component, fracture can occur [44].

- *Failure during rapid thermal cycling.* Thermal gradients arising during rapid heating or cooling can generate out-of-plane bending stresses that may lead to failure in one of the brittle components in the ceramic-to-metal joint. In addition, thermal cycling may lead to fatigue problems in both the metals and ceramic components. Specifically in ceramic materials, this can occur due to a critical size under even small thermally generated stresses.

- *Failure upon thermal aging.* As the glass begins to crystallize, its carefully engineered thermal expansion properties will change and continue to evolve with time at operating temperature, which can ultimately limit the number of thermal cycles and the rate of cycling at which the joints are capable of surviving [7]. In addition, compositional and microstructural changes induced by long term thermal diffusion are likely to take place at the seal/substrate interfaces, which may also lead to seal degradation and subsequent failure.

Despite of the above-discussed problems, glasses and glass-ceramics have been focused on as the potential sealing materials with major emphasis on alkaline earth aluminosilicates [1, 43, 44, 46] borosilicates, and lanthanide alumino borosilicates [12, 1, 3, 45-47] Of course, the effect of many other glass additives have been evaluated and the glasses have been tailored using various additives in accordance with the required properties [9, 7, 5, 47].

3.32 Criteria for selecting suitable Glass Sealant:

Different network formers, modifiers, intermediate and additives used in it. The effect of all these variables on the properties of glasses has been considered as follows:

- **B_2O_3: SiO_2 ratio**

B_2O_3/ SiO_2 ratio is a dominant factor in determining the glass transition temperature, T_g and the viscosity versus temperature behaviour of the glasses [3, 46, 50]. Glasses with high B_2O_3/ SiO_2 ratios have T_g at the lower end while those with low B_2O_3: SiO_2 ratios decrease glass transition temperature. Decrease in TEC of the glasses on increasing the SiO_2 content has also been reported by Lara et al. [50].

- **Crystallization of glasses**

The extent of crystallization is the major factor in the glass. Glass–Ceramics, which can be prepared by controlled crystallization of glass, possess superior mechanical properties and have very different thermal expansion coefficients (TEC), due to nucleation of different crystalline phases in different volume fraction. To develop a good sealant, it is therefore, necessary to understand the crystallization kinetics with other components of the cell [50]. In the case of barium-containing glass-ceramics for SOFCs, the crystallization increases thermal expansion. The crystallization in barium glass ceramics foe SOFC will increase the thermal expansion.

- **Effect of additives**

The properties of the sealants vary considerably by the use of several additives. The choice of additives is restrictive as they do not influence just one property of the sealant but they also have various side effects. Al_2O_3, for example, improves flux, thus making for better joining behaviour. On the other hand, too much Al_2O_3 decreases the thermal expansion, as it promotes the formation of a crystalline phase, which exhibit low thermal expansion coefficient [55]. Similarly, Na_2O acts as the most effective flux, but it makes the glass soluble in water. Na_2O can be replaced by K_2O but the alkali cations react vigorously with the fuel cell components like cathode and form undesirable low

TEC phases [3, 46, 50]. The effects of various additives on the properties of sealants are listed in below in Table 2.

Table 2: Effect of additives [3, 4, 5, 48, 47, 51, 52-54]

Additive	**Effect**
Al_2O_3	Improves flux, thus making for better joining behaviour. Prevents rapid crystallization of glass during heat treatment and also increase surface tension of glass. Too much Al_2O_3 decreases thermal expansion as it promotes the formation of crystalline phase with low TEC.
Na_2O, K_2O	Act as effective flux but the alkali cations react vigrously with the fuel cell components like cathodes; have undesirable TEC. Increases conductivity
La_2O_3, Nd_2O_3, Y_2O_3	Increase TEC, T_g, T_M
B_2O_3	Improves flux, reduces T_g, surface tension and stability of glass
ZnO, PbO	Improves flux, reducing agent
Cr_2O_3, V_2O_5	Reduces surface tension
NiO, CuO, CoO, MnO	Improves adhesion
TiO_2, ZrO_2, SrO, MgO, Cr_2O_3, Ni	Stimulates crystallization
Sb_2O_5	Oxidizing agent

CHAPTER 4

LITERATURE REVIEW

4. Literature Review:

It has been observed that the TEC of BaO-MgO-SiO_2 and BaO-ZnO-SiO_2 increase with increasing BaO content for constant SiO_2 contents [50]. This increase in TEC is due to the formation of barium silicate ($BaSiO_3$), which has large TEC, as compared to, for example, enstatite ($MgSiO_3$). Barium aluminosilicates glass-ceramics crystallize to form celsian ($BaAl_2Si_2O_8$) in addition to, or instead of barium silicate [5, 6, 46, 55, 56]. The two common forms for celsian, monoclinic and hexagonal have very different TEC. Hexacelsian provides the high TEC for SOFC applications, while monocelsian has a very low TEC. For some compositions, silica (quartz or cristobalite) can also form. Cristobalite is particularly problematic due to a displacive transformation upon cooling with an associated volume decrease, which may cause cracking [1]. Calcium oxide is often added to barium aluminosilicates glasses to form barium-calcium aluminosilicates (BCAS) sealants, in which, an additional phase, barium calcium orthosilicate ($Ba_3CaSi_2O_8$), with a desirably large TEC is formed during crystallization [2, 55]. The interaction of the BCAS sealing glasses with various types of interconnect materials has been studied by various research groups [60-62]. Reactions of BCAS glasses are more prevalent with the interconnect materials, primarily due to chromium, which is typically present in both ceramic and steel interconnect materials. Of the commonly used alkaline–earth oxides, silicates containing barium oxide are the most reactive [6, 7, 63] and those containing magnesium oxide are the most adherent [64]. The interfaces between silicates containing magnesium or calcium and chromium forming alloys have been observed to contain $MgCrO_4$ [39] or $Ca_3Cr_2Si_2O_8$ [6, 64, 65] respectively. However, the reaction is more extensive in barium containing silicates, which, even with the presence of calcium in barium calcium aluminosilicate [2, 6, 57, 58, 51] form $BaCrO_4$. Thus, the improvements in thermal expansion matching provided by barium additions are balanced with increased reaction with the interconnect material.

Larsen and James [58] also reported that presence of Cr (VI) in the form of $CaCrO_4$ might cause pore formation inside the seal if severe reaction takes place at the interface. This may not only create leakage in the seal but will also reduce the mechanical strength.

In general, the long term stability of the interconnect is critical parameter for electrical performance. But the chemical reaction for the sealing glass with an oxide scale appears to be critical for the hermiticity requirement [3].

Ley et al. [3] has reported promising results for high B_2O_3 glasses in the SrO-La_2O_3-Al_2O_3-B_2O_3-SiO_2 system. However, the softening temperature of these glasses was too low for SOFCs operating above 700^oC [67]. Also, glass compositions based on B_2O_3 tend to exhibit excessive volatilization in the SOFC environment. P_2O_5 based glasses can be adjusted to minimize volatilization but their TECs are too low and they have low mechanical strength [4]. To date, the best results have been obtained using compositions rich in silica. While alkali silicate glasses tend to be very reactive towards SOFC components [46], alkaline-earth aluminosilicates glasses have yielded promising results [49-54].

Imanaka et al. [68] examined the effect of ceramic additions containing Al, such as alumina, aluminum nitride, mullite and spinel into the borosilicate glass for suppression of cristobalite precipitation. The results showed that mullite or aluminum nitride suppress cristobalite formation more effectively than alumina or spinel. Although both follow a simple rule of mixtures, glass/mullite composites can be fabricated with the lower dielectric constants than glass/alumina composites, while maintaining a thermal expansion coefficient close to Si.

Lahl et al. [5-7] and Bahadur et al. [49] have studied influence of alkaline earth metals A (A=Ba, Ca, Mg) and nucleating agents (TiO_2, ZrO_2, Cr_2O_3 and Ni) on the crystallization kinetics of AO-Al_2O_3-SiO_2-B_2O_3 glasses by thermal and microstructural studies. The activation energy of crystal growth, E_a, was shown to be varying between 330 and 622 kJ/mol. It was observed that E_a increases with nucleating agents except ZrO_2. An increase of the Al_2O_3 concentration induced phase separation and decrease in E_a. Also, chemical interactions of the candidate sealants with 8-mol% yttria stabilized zirconia (8YSZ), Ni and the oxide dispersion strengthened (ODS) alloy was studied. It was observed that MgO base sealants exhibit superior properties as compared to BaO and CaO base sealants because of higher activation energy of crystal growth thereby hindering crystallization and moderate chemical interactions. Also it was reported that glasses with TiO_2 as nucleating agent are known to have a high tendency for the formation of ordered zones

with high TiO_2 content due to high field strength of Ti^{4+}, which can cause phase separation and nucleation. The most encouraging result was the complete absence of cordierite phase ($Mg_2Al_4Si_5O_{18}$) in all powder mixtures composed of the sealant with Cr_2O_3 as the nucleating agent. High values of T_g, T_c, and the activation energy of crystal growth is obtained if Cr_2O_3 (0.6 mol %) is used as nucleating agent. The chromium seemed to have a thermodynamic affinity to magnesium, which favours spinel formation and suppresses the formation of the cordierite phase in many powder mixtures

CHAPTER 5

EXPRIMENTAL TECHNIQUES

5.1 Sample Preparation:

The brief detail about sample processing methodology which we followed during the course of investigation is presented in this chapter.

Samples of the glass were prepared by mixing of the raw materials in the form of SiO_2, B_2O_3, Y_2O_3, Al_2O_3, La_2O_3, MgO and SrO using conventional melt-quenching techniques. The purity of constituent oxides which were used to prepare the samples was ≥ 99 mol%. Each batch was prepared by mixing an appropriate mole fraction of well desired initial ingredients using mortar and pestal. Sample compositions with their label are given in table 3.

Table 3 : Glass compositions (mol %) with their label

Sample Label	**SiO_2**	**B_2O_3**	**SrO**	**MgO**	**Y_2O_3**	**La_2O_3**	**Al_2O_3**
VS1	40	20	30	0	10	0	0
VS2	40	20	30	0	0	10	0
VS3	40	20	30	0	0	0	10
VM1	40	20	0	30	10	0	0
VM2	40	20	0	30	0	10	0
VM3	40	20	0	30	0	0	10

The mixed powder of these samples were placed in recrystallized alumina crucible and melted in an atomized Molybdenum Disilicide ($MoSi_2$) electric resistance furnace. The powder of the samples were initially kept at 1000ºC for 1 hour for calcination to occur and release of water from the starting materials then they were reheated at 1550ºC and

kept at this temperature for half an hour in order to achieve the homogeneity. The schedule for sample melting is shown in figure 5.1. The melt was poured either in graphite mold or on the flat copper plate and quenched by other copper plate in air to obtain flakes. All the samples were prepared using the route described above. The details of the sample preparation and other relevant information about preparation and characterization are summarized in the figure 5.2.

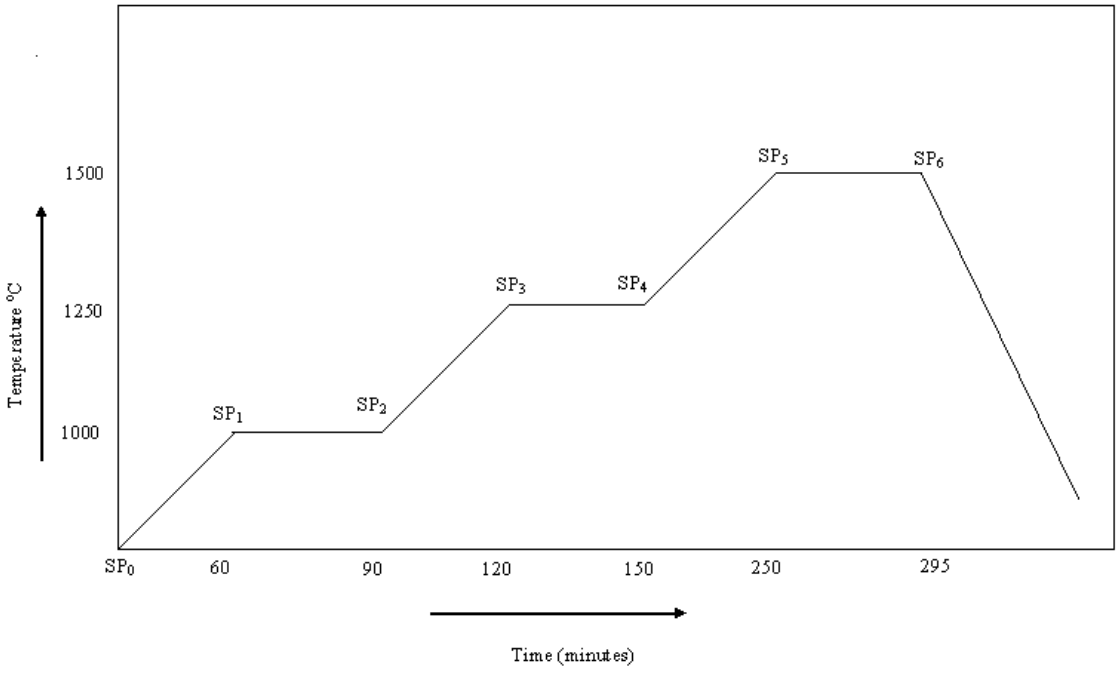

Fig. 5.1 Typical schedule followed for the melting of the glass samples.

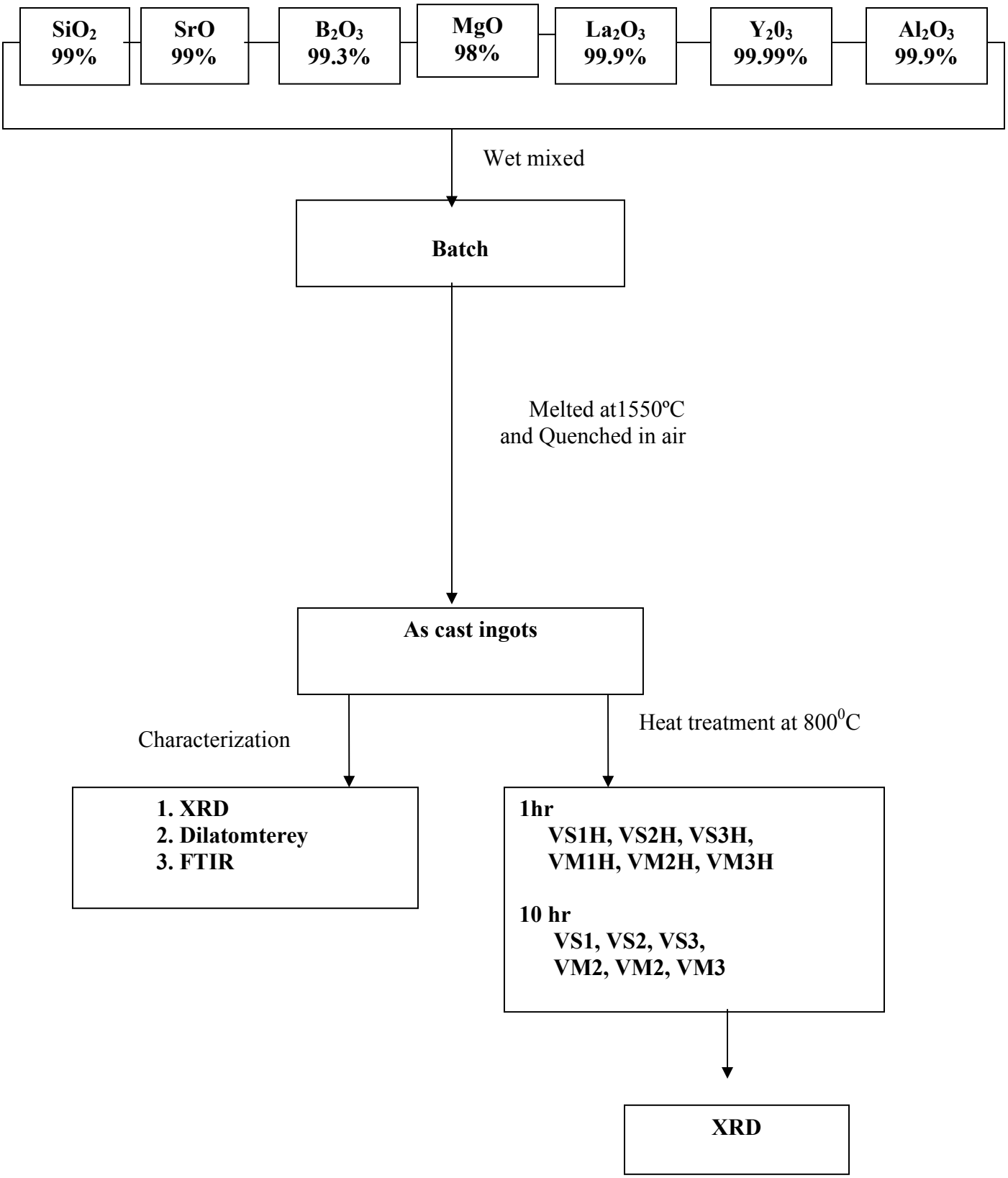

Fig. 5.2 Typical flow chart showing the path followed for the preparation and characterization of the glass samples

5.2 X-ray diffraction technique:

X-ray diffraction analysis (XRD) is a non-destructive, very versatile technique to determine the crystalline phases and their volume fractions. The sample is irradiated with monochromatic X-ray and the reflected radiation is recorded by the counters. In this technique various forms of the samples could be used and very less amount is required for phase determination.

The X-ray diffraction patterns were recorded using Rigaku model Geiger diffractogram with CuK_α radiation (λ = 1.5418Aº) obtained from copper target using an in built Ni filter. The 2θ values for XRD patterns were generally taken in the range of 5º to 100º for most of the samples at a scan speed of 5 degree per minute. The inter planar spacing (d) values of samples were calculated using the Bragg's law.

$$2d \sin \theta = n \lambda \qquad (1)$$

Where λ is the wavelength of incident X-ray, d is the interplanar distance and θ is diffraction angle. The XRD patterns were identified using Powder Diffraction files (PDF). The geometric representation of Bragg's law is given in figure 5.3.

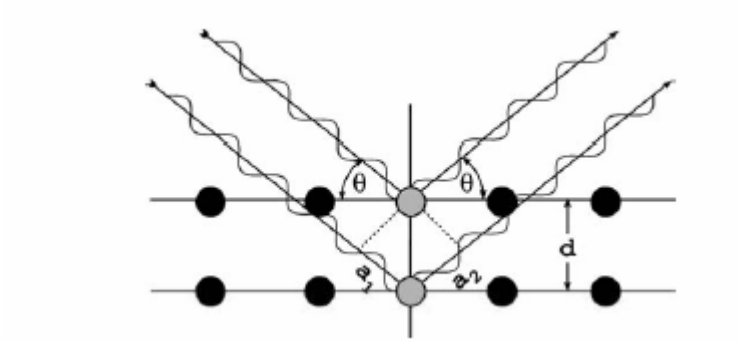

Figure 5.3 Geometric derivation of Bragg's law: constructive interference occurs when the delay between the waves scattered from adjacent lattice planes given by $a_1 + a_2$ is an integer multiple of the wavelength λ

5.3 Fourier Transform Infrared Spectroscopy (FTIR):

Infrared (IR) spectroscopy is one of the most common spectroscopic techniques used to characterize organic and inorganic materials. Simply, it is the absorption measurement of different IR frequencies by a sample positioned in the path of an IR beam. The main goal of IR spectroscopic analysis is to determine the chemical functional groups in the sample. Different functional groups absorb characteristic frequencies of IR radiation. Using various sampling accessories, IR spectrometers can accept a wide range of sample types such as gases, liquids, and solids. Thus, IR spectroscopy is an important and popular tool for structural elucidation and compound identification.

5.3.1 Parts of FTIR Spectrometer

An IR spectrometer consists of three basic components: monochromatic radiation source, monochromatic sample holder and detector. A schematic diagram of a typical dispersive spectrometer is shown in figure 5.4

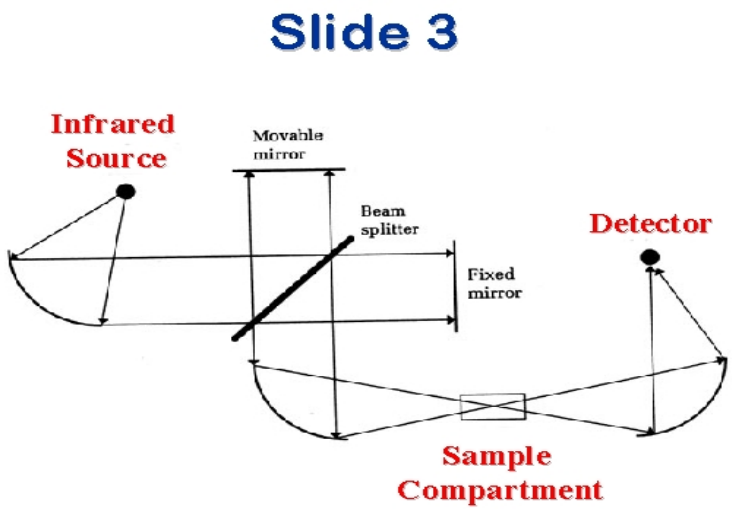

Fig. 5.4 Ray diagram of FTIR

IR Frequency Range and Spectrum Presentation

Infrared radiation spans a section of the electromagnetic spectrum having wave numbers from roughly 13,000 to 10 cm^{-1}, or wavelengths from 0.78 to 1000 µm. It is bound by the red end of the visible region at high frequencies and the microwave region at low frequencies.

IR absorption positions are generally presented as either wave numbers or wavelengths (λ). Wave number defines the number of waves per unit length. Thus, wave numbers are directly proportional to frequency, as well as the energy of the IR absorption. The wave number unit (cm^{-1}, reciprocal centimeter) is more commonly used in modern IR instruments that are linear in the cm^{-1} scale. In contrast, wavelengths are inversely proportional to frequencies and their associated energy. At present, the recommended unit of wavelength is μm (micrometers), but μ (micron) is used in some older literature.
IR absorption information is generally presented in the form of a spectrum with wavelength or wave number on the x-axis and absorption intensity or percent transmittance on the y-axis.

5.4 Dilatometerey:

A dilatometer measures the expansion of a material when it is heated. A small sample of the material is placed into the instrument and then heated (or cooled) according to a schedule picked by the investigator.

5.4.1 Working Principle of dilatomterey

In a dilatometer the dimensional change is measured by subjecting a sample to a change in temperature. The need for these members is a practical one, since the transducer that registers this change cannot normally be subjected to the same temperature excursion as the sample. The closer the transducer can be coupled to the sample, the less the transmission member can influence the results, and, consequently, the more ideal the dilatometer becomes. Specifically, the more one can reduce the contributions made by any such intervening machine members, the more purely the data will represent true values.
In principle, one can devise a simple arrangement in which the movement is transmitted out of the controlled environments and into the ambient by holding the sample between two rods which extend outside of the heated region as shown in figure 5.5. The sample pushes the two rods (A and B) as it is being heated, hence the name "pushrod". The sample will expand an amount shown by the shaded area, ΔL_S. By examining the experimental model, it becomes immediately clear that this configuration will not

produce the desired ΔL_S. Since portions of both rods A and B are in the controlled environment, it is inevitable that they themselves will also expand (ΔL_A and ΔL_B respectively). Thus, the measured value of (ΔX_A+ΔX_B) will contain (ΔL_A+ΔL_B) in addition to ΔL_S. The sample's length change, ΔL_S, can therefore be written as:

$$\Delta L_S = (\Delta X_A - \Delta L_A) + (\Delta X_B - \Delta L_B) \text{ ……(2)}$$

Unless one can assign values to ΔL_A and ΔL_B, the true magnitude of ΔL_S cannot be determined from the measured values of ΔX_A and ΔX_B alone. Obviously, if ΔL_A and ΔL_B are not present at all, the measurement becomes absolute, but as long as this is not the case, the measurement is, in principle, a relative one.

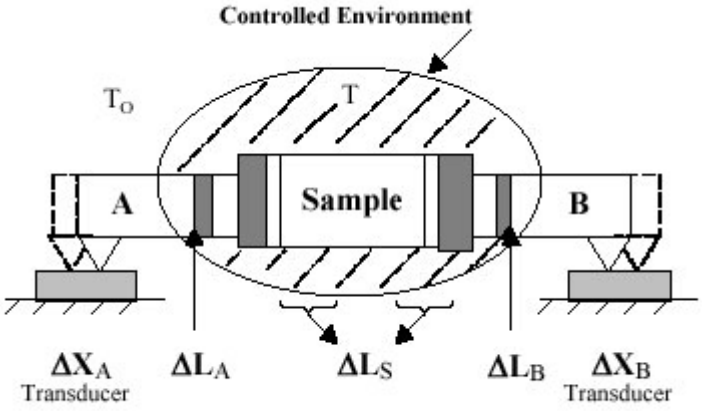

Fig. 5.5 Diagrammatic representation of sample holder (top view)

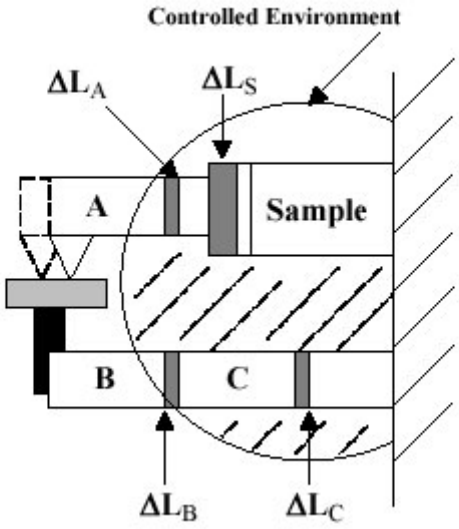

Fig. 5.5 Diagrammatic representation of sample holder (side view)

The most tempting prospect is to minimize the magnitudes of ΔL_A and ΔL_B in comparison to ΔL_S and then to neglect them. If the material of rods A and B do not expand appreciably compared to the sample, or not at all, the conditions become favourable to obtain results with reasonable accuracy. A good example of this would be to use light beams that do not expand when entering the controlled environment in place of rods A and B. More frequently, very low expansion materials such as fused silica are used for rods A and B, and, for many applications, this is enough to reduce inaccuracies to a small fraction of the measured values when high expansion materials such as plastics are tested.

In general usage, however, one must determine the magnitude of ΔL_A and ΔL_B accurately. Most commonly, one tests a sample from a material already well-defined by some other absolute method (twin telescopes, interferometer, etc.), which then leaves only the combined values of ΔL_A and ΔL_B unknown. This process is known as "calibration" for the dilatometer; the well-defined material is referred to as a "standard" or "reference;" and the combined value of ΔL_A and ΔL_B and is known as "system correction." Upon closer examination, it is clear that the correction obtained with a standard will be true only if this sample is of the same length, ensuring that the

protruding lengths of rods A and B into the controlled environment region are identical during the calibration and during the test. Furthermore, what may be true at one value of temperature T may not be true at another. To ensure that a calibration is indeed applicable: the sample and reference lengths must be close to each other. The calibration thermal cycle must closely approximate the test cycle (or vice versa). The reference's expansion must be close to the expected expansion of the sample. Differential dilatometers usually measure very small differences with high magnification. A major drawback of this configuration is its susceptibility to errors due to transducer gain misadjustments or malfunctions. As an extreme condition, one can obtain seemingly valid data (that is, the sample appears to expand exactly at the same rate as the reference) with the transducer literally turned off. Additionally, the high magnification severely restricts the range of measurable displacement. For these reasons, the use of differential dilatometers should be limited to applications in which the advantages clearly outweigh these drawbacks. If a temperature change from T_O to T has caused this expansion in a sample of initial length L_O, the average coefficient of linear thermal expansion can be calculated as follows

$$a = (\Delta L_S / \Delta L_O)/(T - T_O) \text{……..Eq.}$$

This coefficient, often referred to as TEC, is only true for the temperature range T_O to T. (Note that the word "linear" should never precede the word "coefficient", as it always implies uniaxial expansion rather than linearity of the coefficient).

Thermal Analysis

Thermal analysis is a technique in which a physical property of a substance is measured as a function of temperature or time while the substance is subjected to a controlled-temperature programme. The two main thermal analysis techniques that are used in the present study are thermogravimetric analysis (TGA) and the differential scanning calorimetery (DSC). TGA gives information about the composition, moisture content and degradation of materials at high temperatures. TGA is a technique by which the mass of a substance is measured as function of temperature or time while the substance is subjected to a controlled temperature programme in a specified environment.

CHAPTER 6

RESULTS AND DISCUSSIONS

6.1 X-ray diffraction analysis:

As described earlier the composition of glasses prepared for the present study is given in table1. These samples were splat quenched in air after melting. All the six categories of the as prepared glasses were found to be amorphous in nature as is evident from the x-ray diffraction pattern as shown in figure 6.1 to 6.6. Even some of the samples were exposed to presence of higher count per second (CPS) but a broad halo peak is observed which is a manifestation of amorphous nature of the samples.

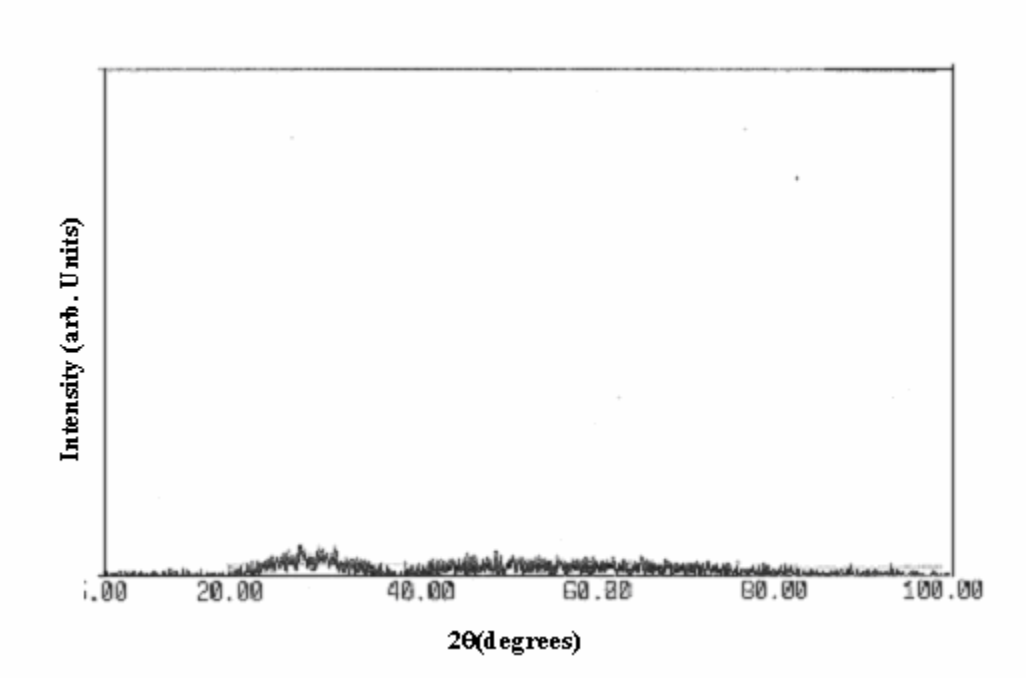

Fig. 6.1 XRD diffractogram for sample VM1

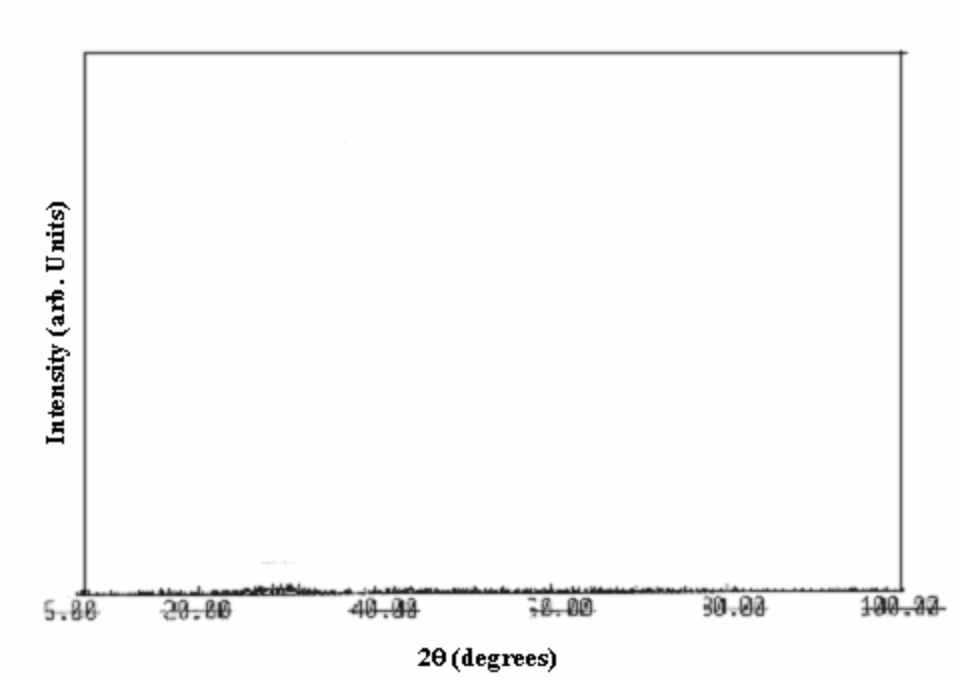

Fig. 6.2 XRD diffractogram for sample VM2

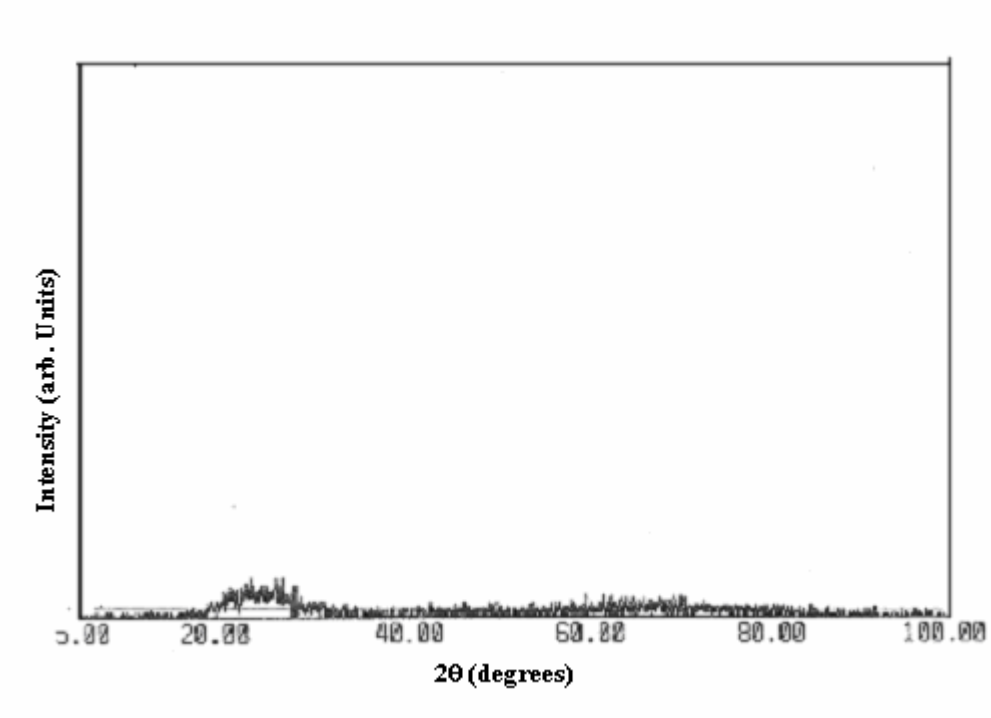

Fig. 6.3 XRD diffractogram for sample VM3

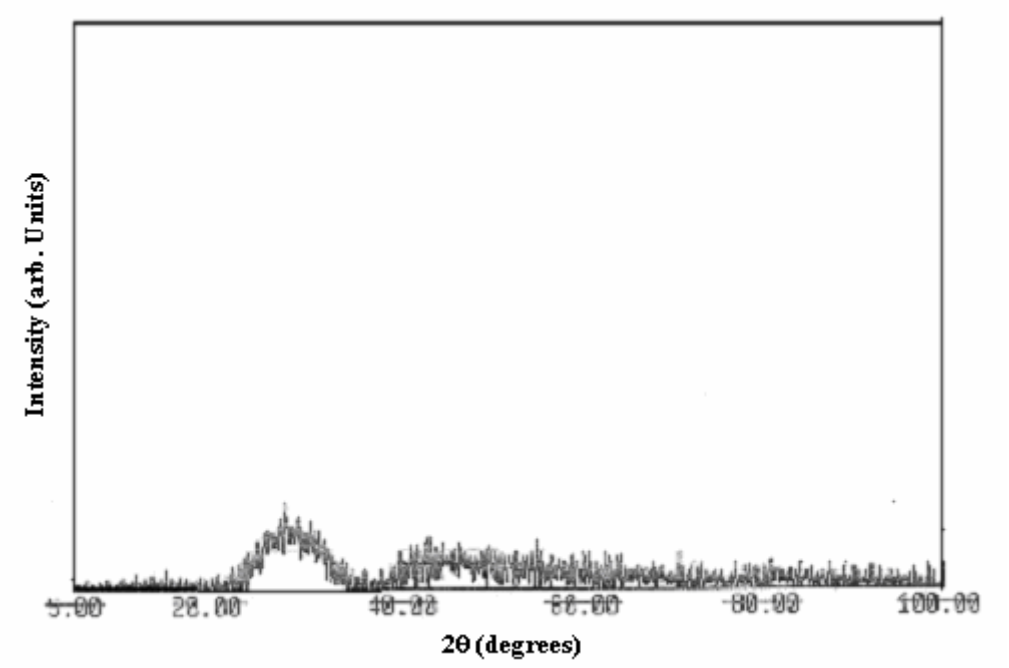

Fig. 6.4 XRD diffractogram of sample VS1

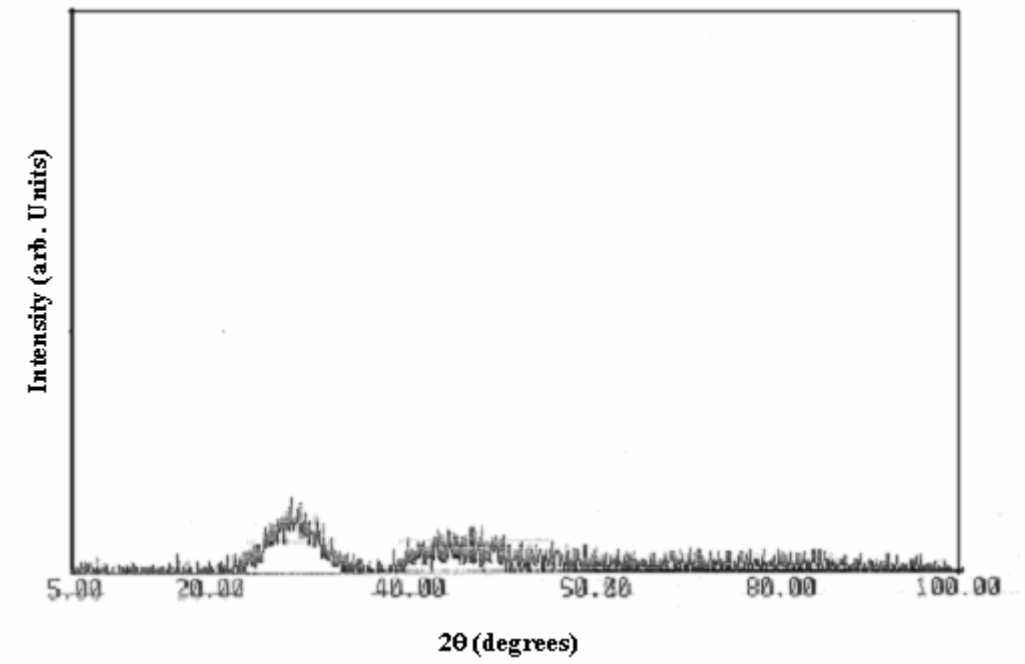

Fig. 6.5 XRD diffractogram for sample VS2

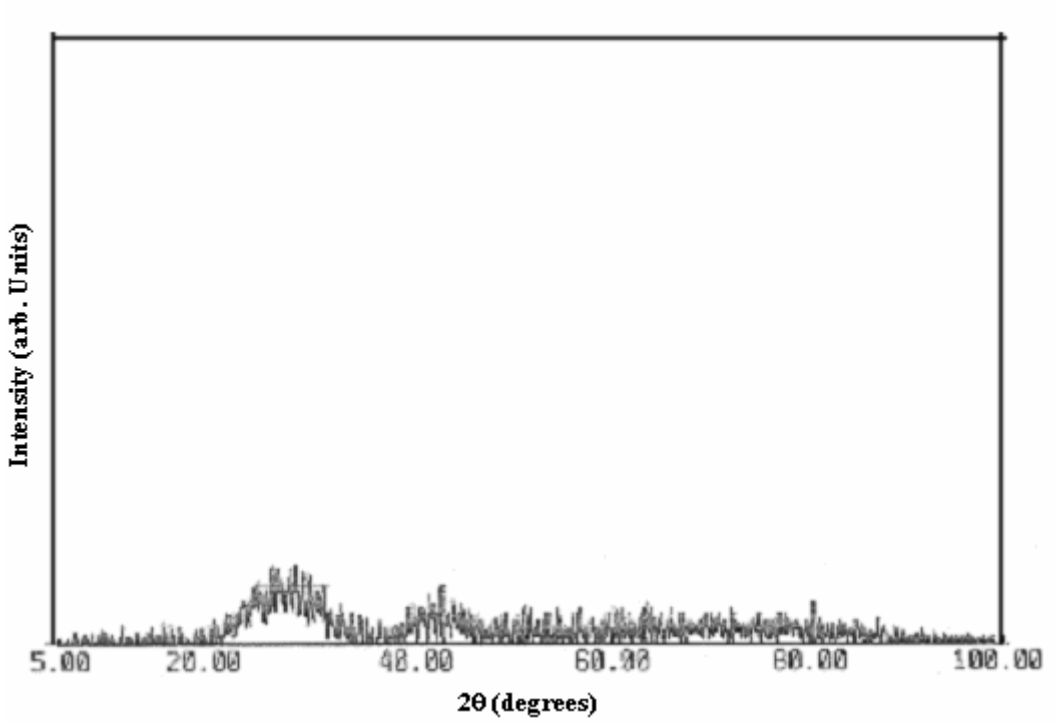

Fig. 6.6 XRD diffractogram for sample VS3

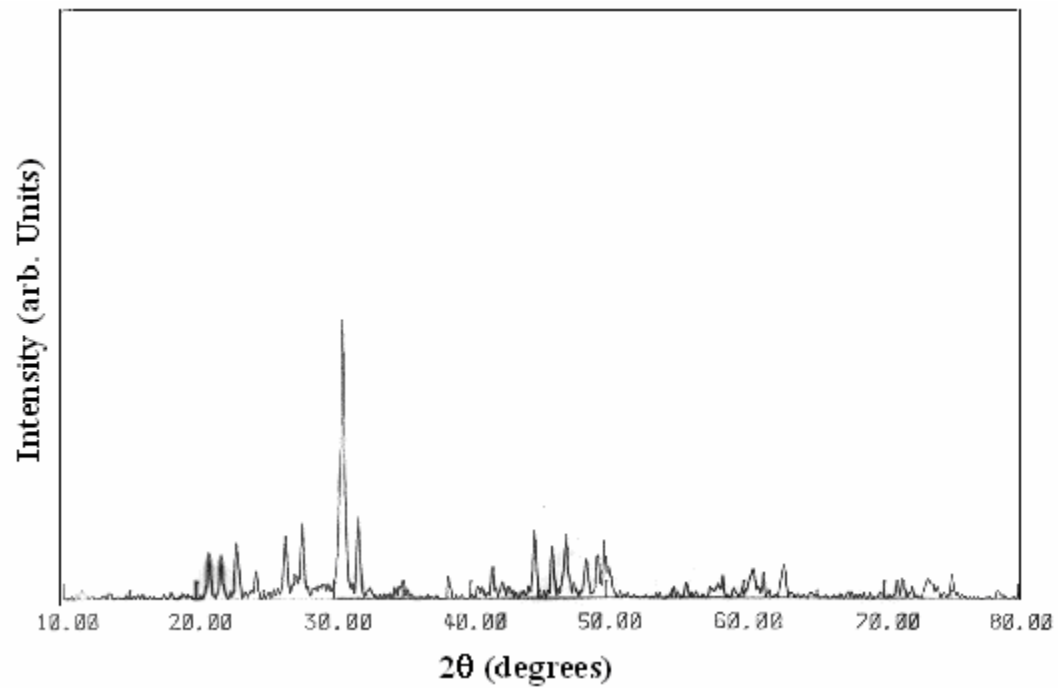

Fig. 6.7 XRD diffractogram for 1 hr heat treated VS2 sample

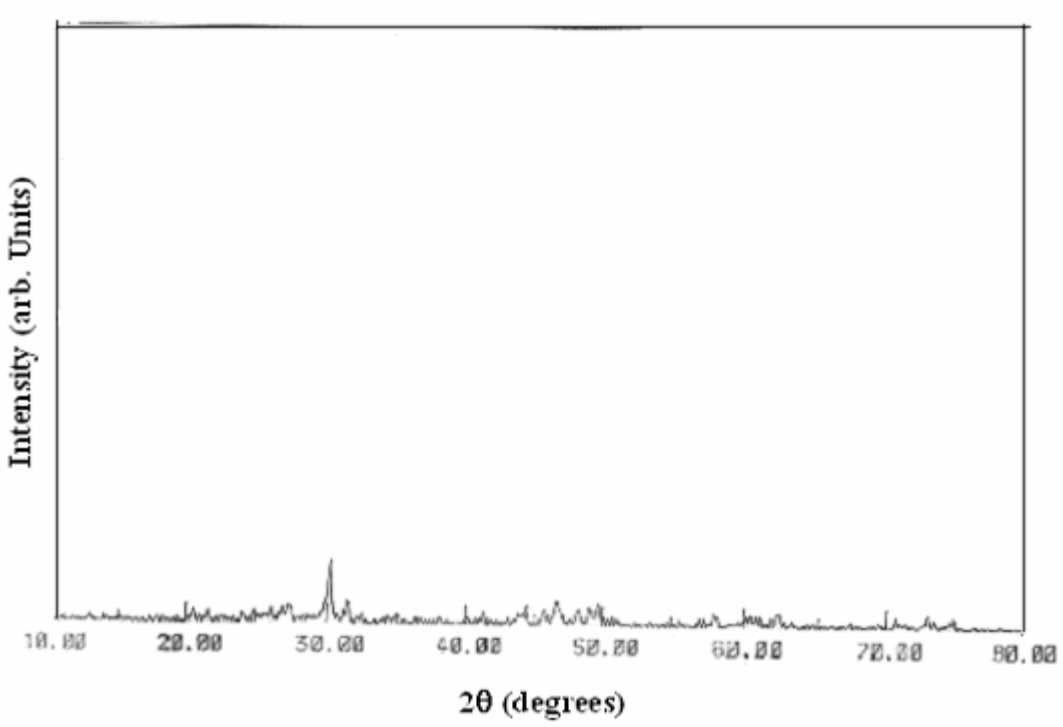

Fig. 6.8 XRD diffractogram for 10 hr heat treated VS2 sample

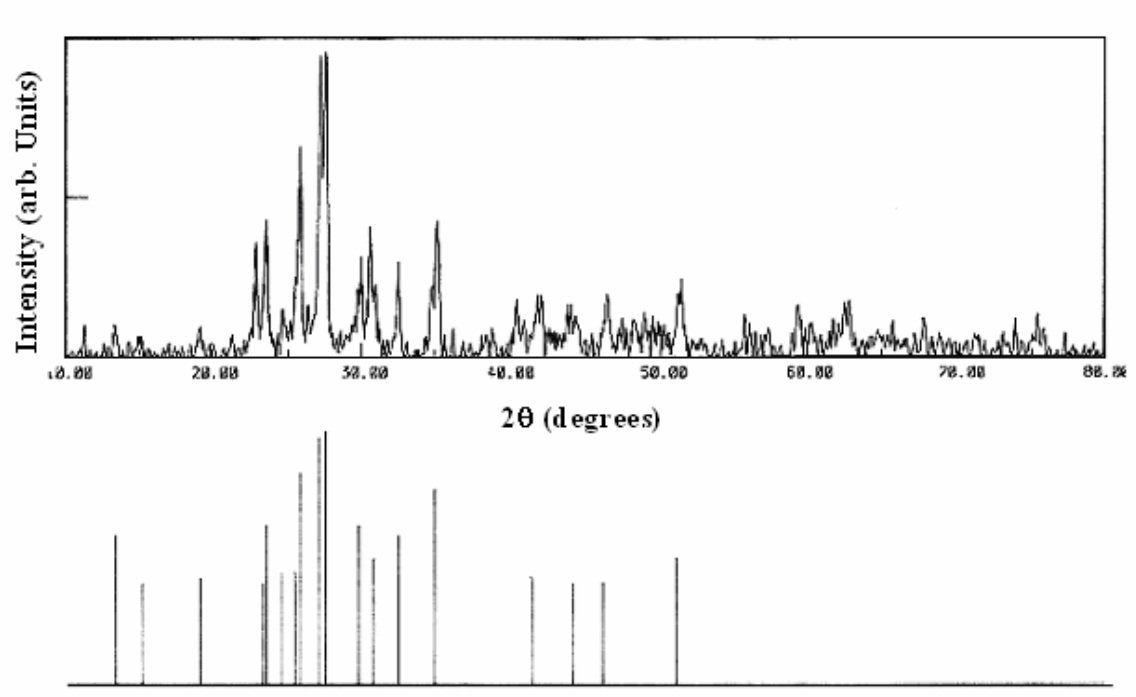

$SrAl_2Si_2O_8$

Fig. 6.9 XRD diffractogram for 10 hr heat treated VS3 sample showing $SrSi_2Al_2O_8$ phase

In order to understand the crystallization kinetics, all the six samples were heat treated at 800ºC for one hour and ten hours respectively. Heat treated samples were examined by the X-ray diffraction to identify the various phase formation with respect to temperature and heat treatment duration. Apart from VS2 sample, all other five samples could not exhibit crystalline phase in 1 hour heat treatment. XRD peaks of this particular sample are not identified with the available powder diffraction files. Moreover, volume of this unknown crystalline phase decreases with increasing heat treatment time as indicated in figure 6.7 and 6.8 respectively. This anomaly may be attributed due to meta stable phase formation initially and in later stage of heat treatment this phase may be changing into more stable phase. According to zdanicwki in SiO_2 based glasses, the early stage of crystallization occurs by formation of a SiO_2 rich solid solution subsequently, in the later stage an isomorphic substitution of 2+ divalent cation and trivalent cation occur at different sites of the unit cell with progressive heat treatment duration [63]. On the other hand, initially (1 hour heat treatment) VS3 sample is not crystallized and in the later stage 10 hours of heat treatment VS3 sample gets crystallized. This crystalline phase is $SrSi_2Al_2O_8$ (celsian) as shown in figure 6.9. Celsian exist in two polymorphs . Hexacelsian is the high temperature phase and monocelsian the low temperature phase .Hexacelsian has hexagonal structure and celsian is monoclinic .The average linear thermal expansion coefficient [63] of hexacelsian is more than celsian phase .The celsian to hexagonal phase change occur at ~ 1590ºC . At temperature 1590ºC hexacelsian is metasable.

It may be attributed due to dissolution of the phase in the glass matrix with increasing heat treatment and time duration. Basically in glass ceramic samples, due to presence of various components in matrix sometimes initially a phase forms in later stages this phase may be converted in more stable phase as the heat treatment duration increases. Similar results have been reported in our earlier studies on MgO based glasses.

6.2 Dilatometerey study:

In dilatomterey studies, the samples show less phase stability and continuous change in thermal expansion coefficient in the table as shown

Table 4: Softening temperature and coefficient of thermal expansion

Sample name	**Ts(ºC)**	**TEC (X 10^{-6}/ºC)**
VS1	650	7.76
VS2	620	5.26
VM1	620	4.7
VM2	730	3.03
VM3	735	1.99

Dilatometer measurements were carried out on some of the glasses in order to determine the glass softening temperature and also find the thermal expansion coefficient (TEC) of the glasses between room temperature to 900ºC. Softening temperature from as TEC are given in table 4 and figures 6.10 to 6.14.

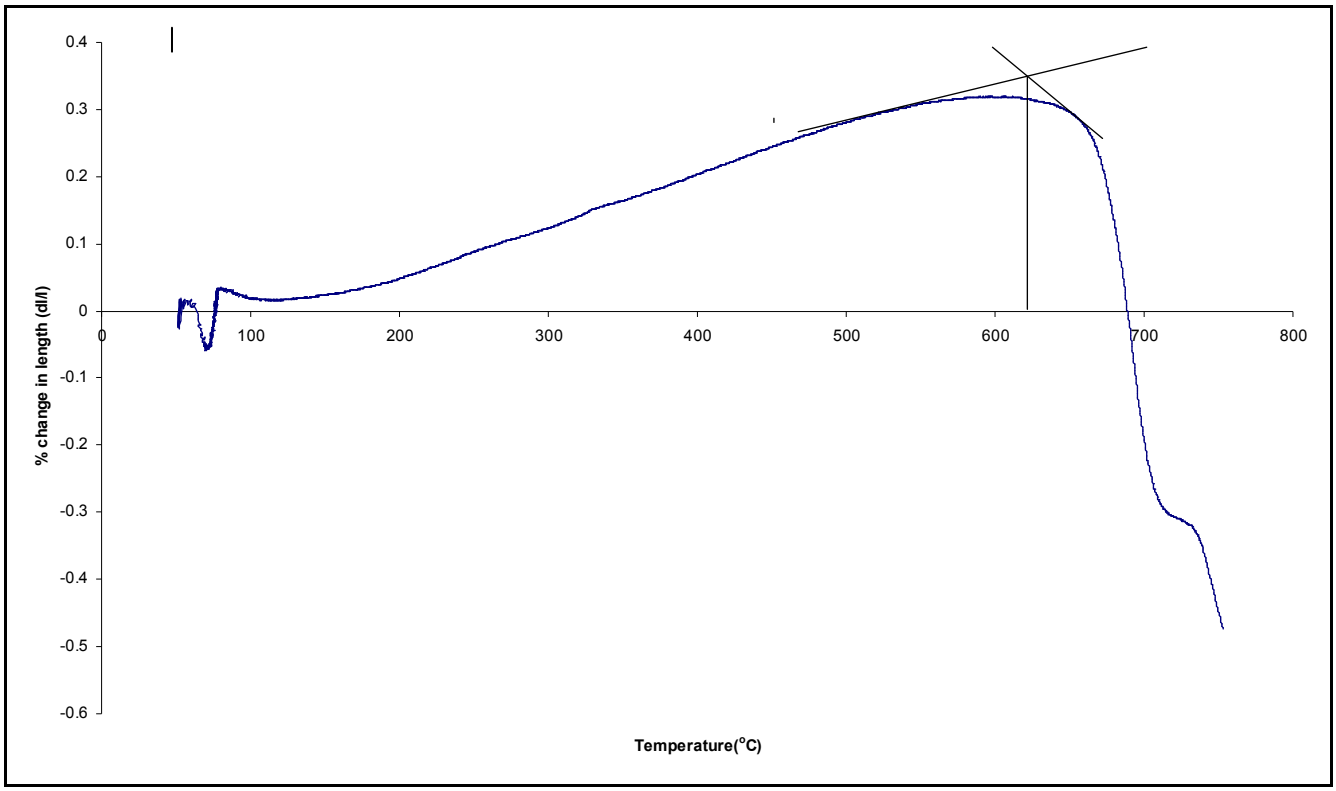

Tg = 620ºC
Ts = 625ºC

Fig. 6.10 Dilatomterey plot of VSI

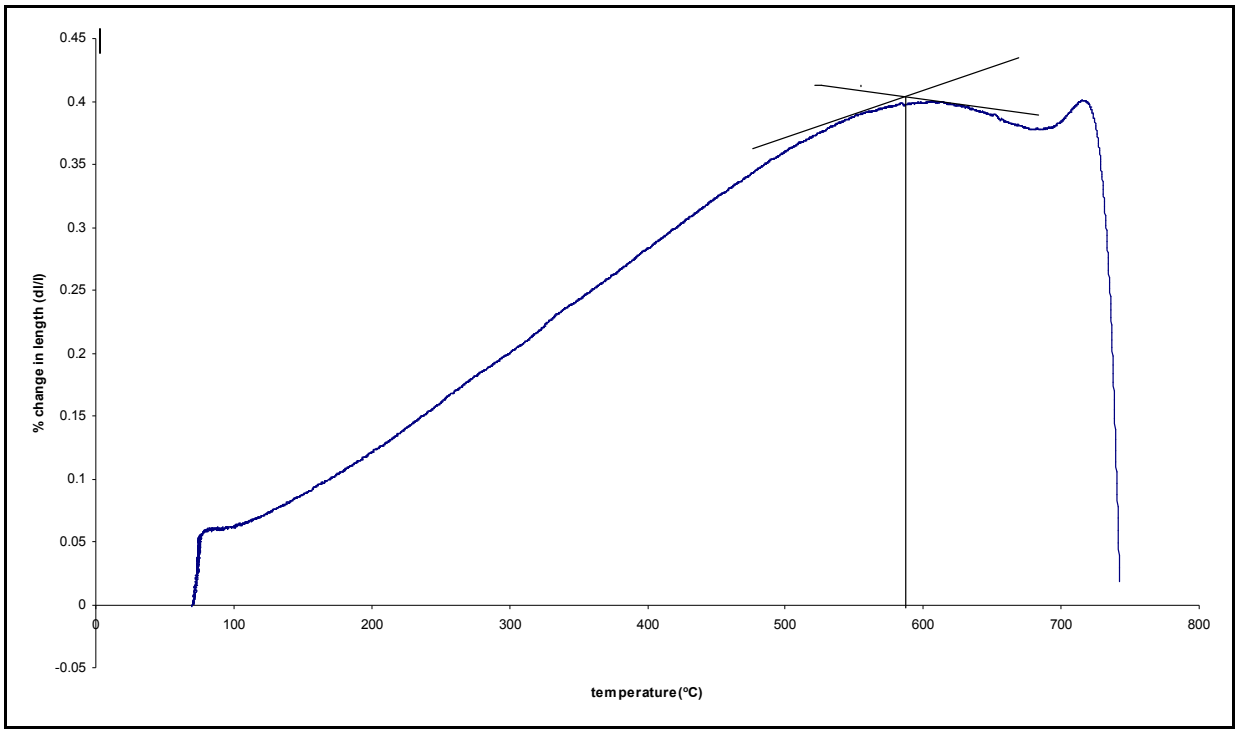

Tg = 590ºC
Ts = 620ºC

Fig. 6.11 Dilatomterey plot of VS2

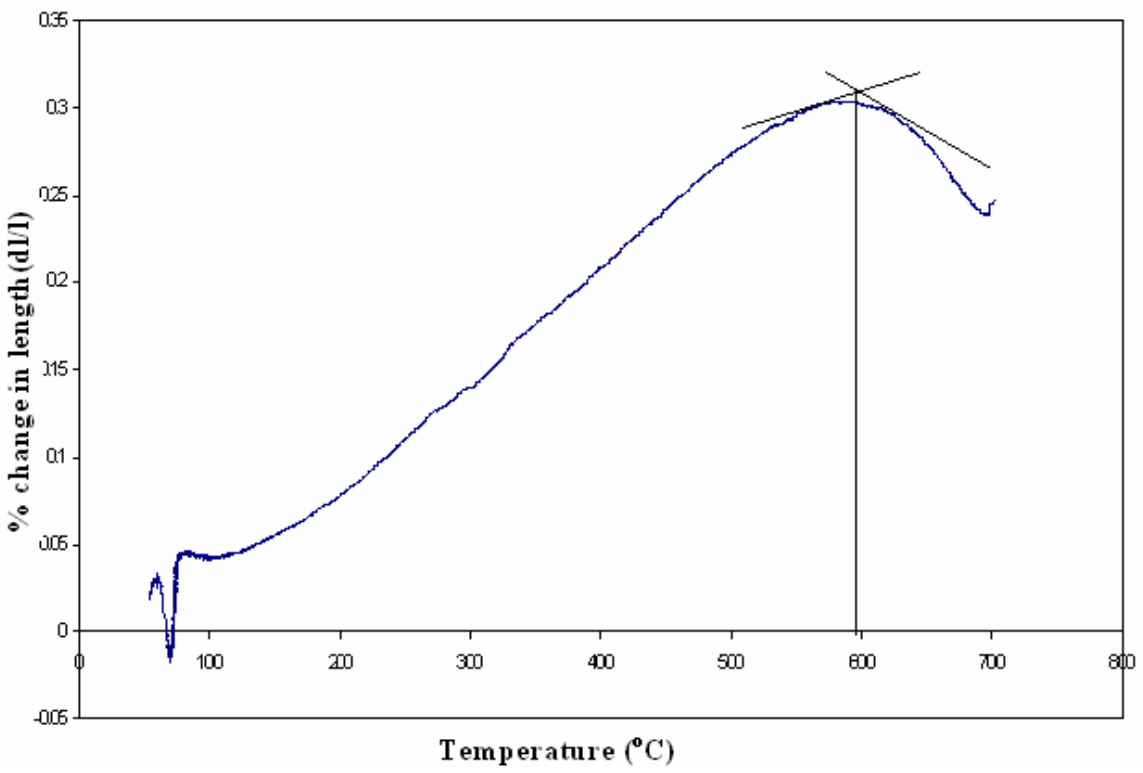

Tg = 595ºC
Ts = 620ºC

Fig. 6.12 Dilatomterey plot of VM1

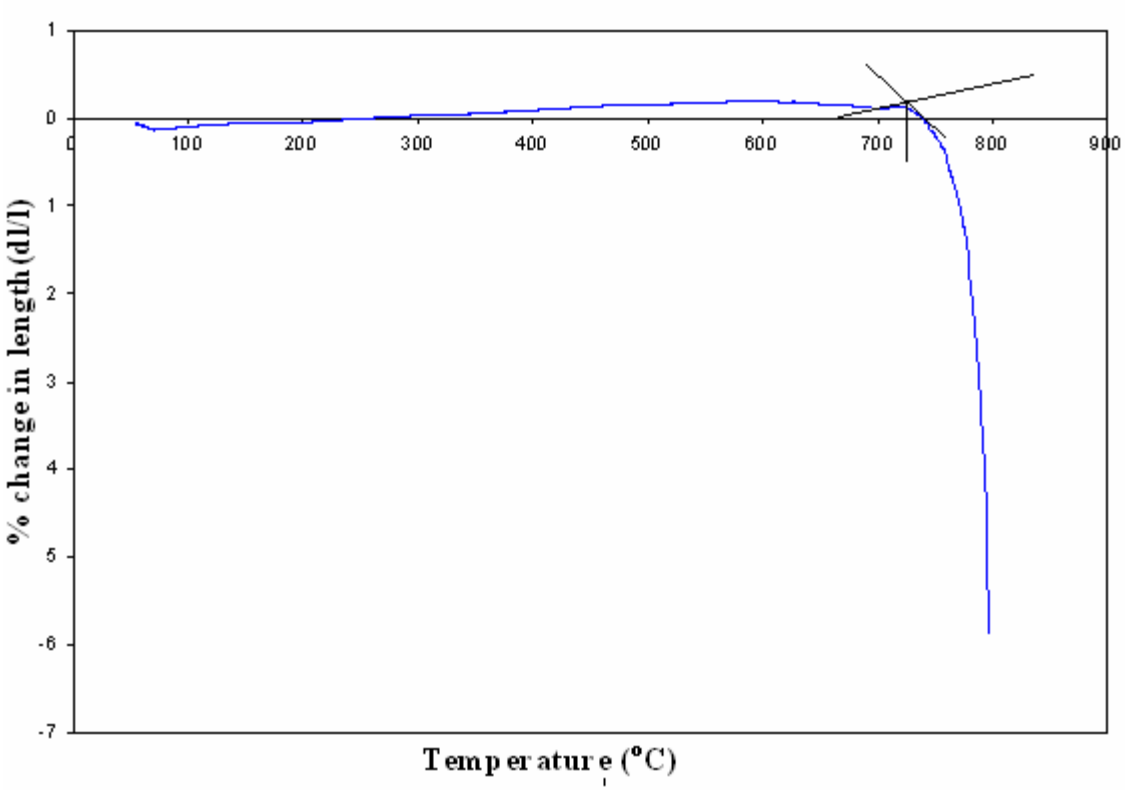

Tg = 720ºC
Ts = 730ºC

Fig. 6.13 Dilatomterey plot of VM2

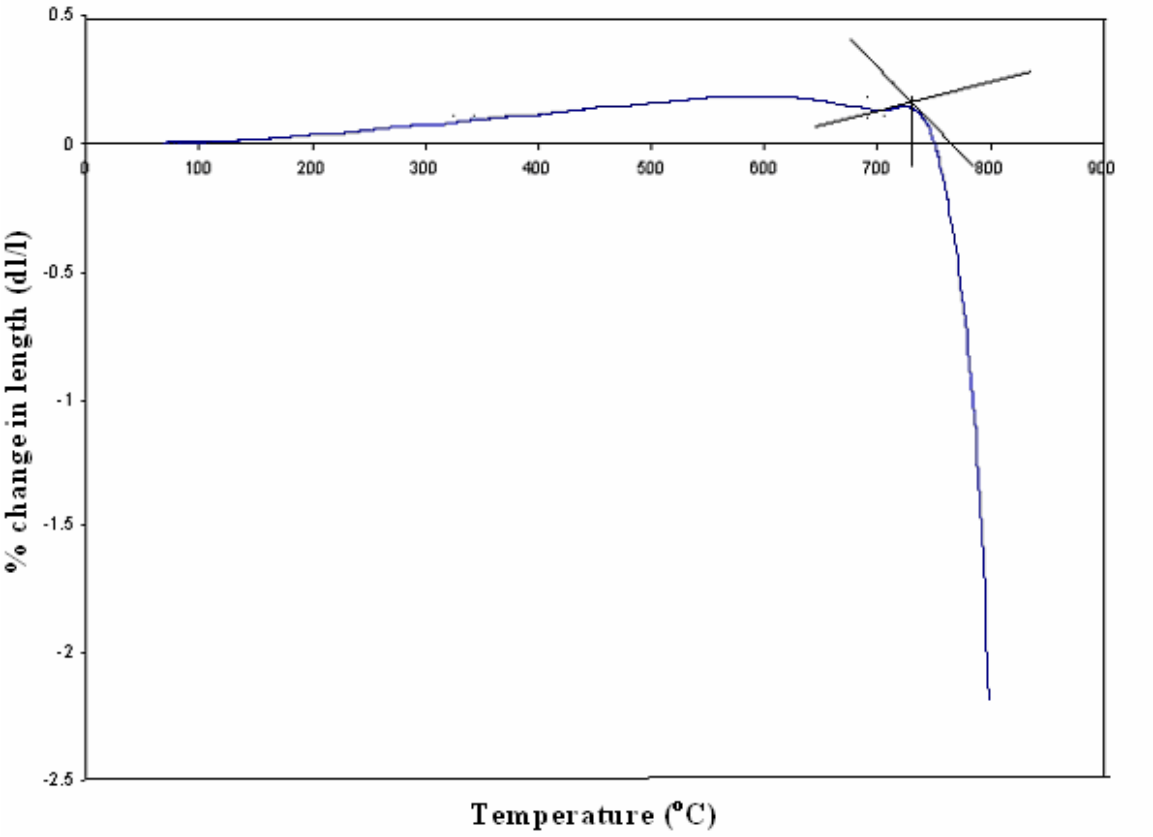

Tg = 720°C
Ts = 735°C

Fig. 6.14 Dilatomterey plot of VM3

The softening temperatures of SrO based samples are lower than MgO based samples. The highest Ts were observed in VM3 samples where Al_2O_3 is present. However the lowest Ts was found in SrO based sample with La_2O_3 content. This can be explained on the basis of field strength of Mg^{2+} and Sr^{2+} , the field strength of Mg^{2+} is more than Sr^{2+} due to this MgO based glasses as compared with SrO based glasses have higher values of Ts. Within SrO based glasses the samples doped with Y_2O_3 have higher T_s as compared to La_2O_3 doped glasses. This can again be explained on the basis of higher field strength of Y^{3+} as compared to La^{3+}. Also looking at the trend being followed by the coefficient of thermal expansion we find that coefficient of thermal expansion (TEC) of VS1 is highest and next is VS2.In case of MgO based samples the TEC follows a decreasing trend i.e. VM1>VM2>VM3 . The SrO based samples have TEC more as compared to

MgO based glasses the reason is that, a very strong glass matrix is formed in case of MgO based glasses due to which bonding is strong in MgO based glasses as compared to SrO based glasses. Thermal expansion of sealants containing SrO is the highest which can be explained by the low field strength of Sr^{2+} ion as compared to those of Mg^{2+} as shown in table 6.

However in case of MgO doped glasses the glass sample doped with Al^{+3} have the highest Ts followed by La^{3+} instead of Y^{3+}. MgO containing glass ceramics, particularly with 10% Al_2O_3, show low thermal expansion partly due to their tendency to form cordierite phase, which is known to exhibit at low value of the TEC [5]. In MgO based sealants, TEC of VM1 sample exhibit higher thermal expansion than sample VM2 though the field strength of Y^{3+} exceeds that of La^{3+}. This might be caused by the higher degree of crystallization tendency of VM1 than VM2 sample as VM1 sample show lower softening temperature than VM2 sample. A typical curve of TGA (VS1) determined with heating rate of 10^{o}C/min is shown in figure 6.15. Besides the glass transition temperature, T_g curve exhibits one exothermic peak indicating the crystallization temperature T_c. VS1 sample show melting above 1050^{o}C. The softening temperature from the dilatometer measurement is compared with the T_g values obtained by TGA. The value obtained by the two different techniques agrees reasonable well.

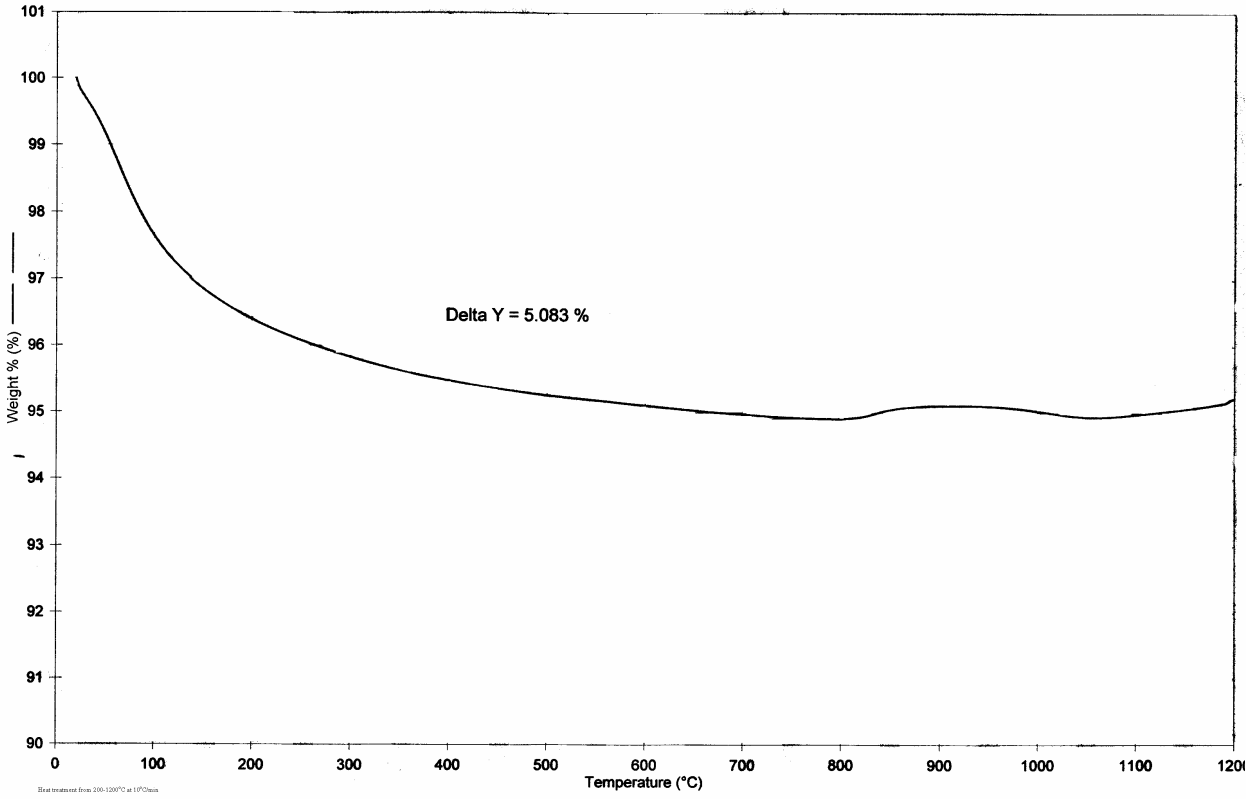

Fig. 6.15 TGA curve for sample VS1

6.3 FTIR Analysis:

Infrared spectrophotometry was carried out on all six glass samples to identify the functional groups present in these samples. In the spectra shown in figures some of the peaks are due to the acetone group and others due to water molecules which have been used during sample preparation. The main peaks are due to borate and silicate groups which are present in higher mol% in the sample. The infrared spectra obtained help us to identify the compound present and the type of stretching (symmetric or antisymmetric) in it. The FTIR spectra of all the six samples are given below in Fig 6.16 to 6.21.

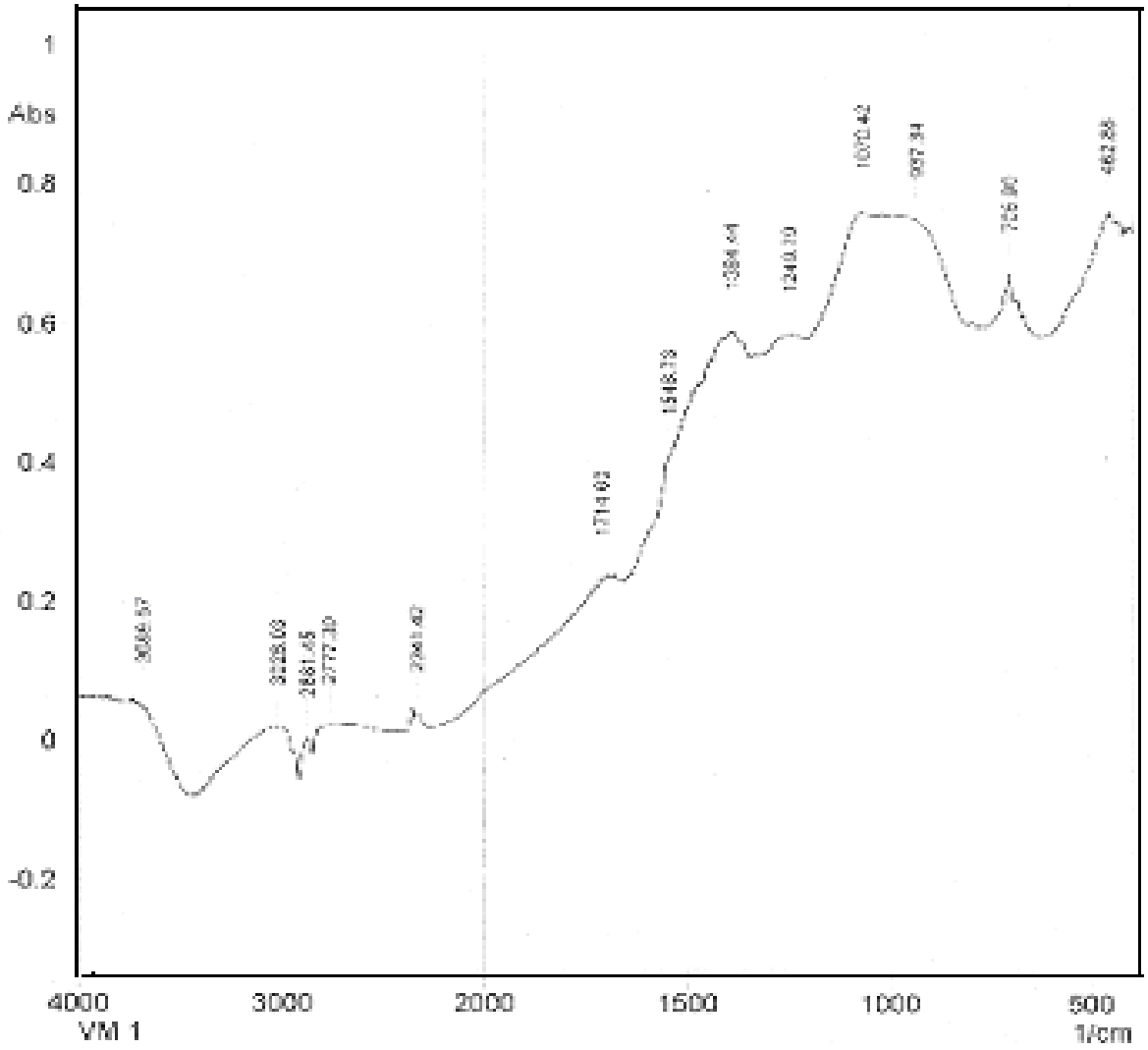

Fig. 6.16 FTIR spectra of sample VM1

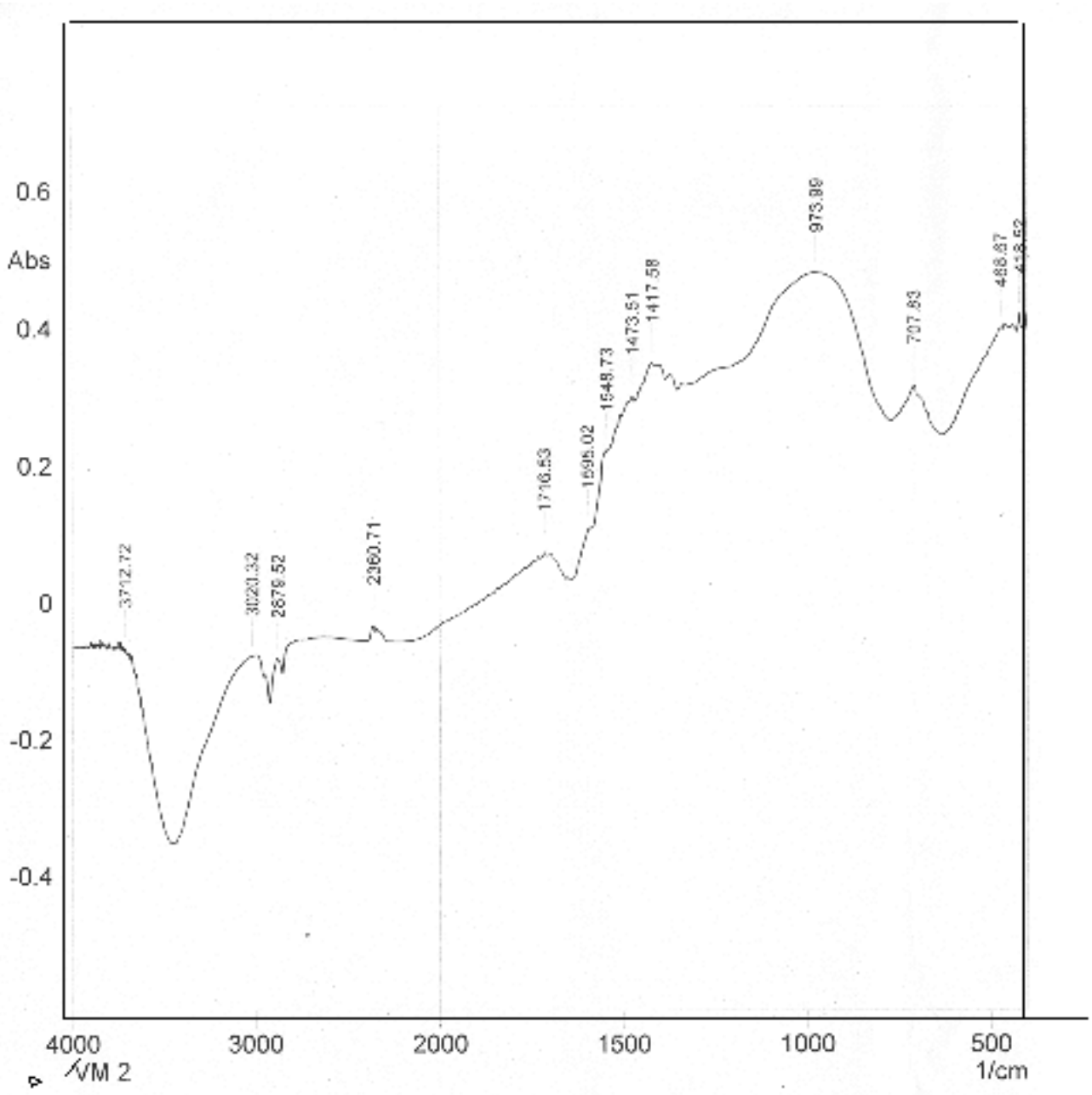

Fig. 6.17 FTIR spectra of sample VM2

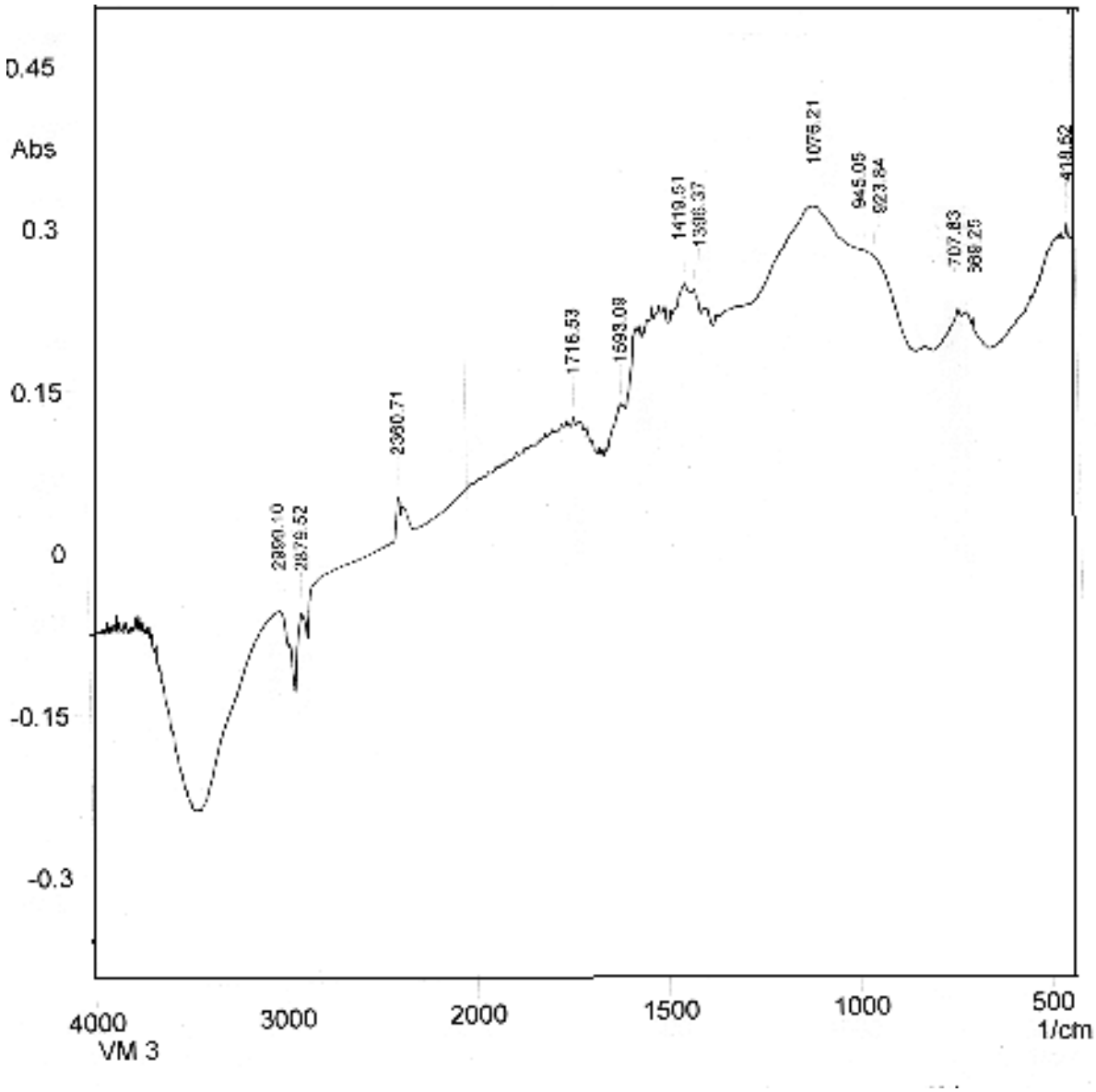

Fig. 6.18 FTIR spectra of sample VM3

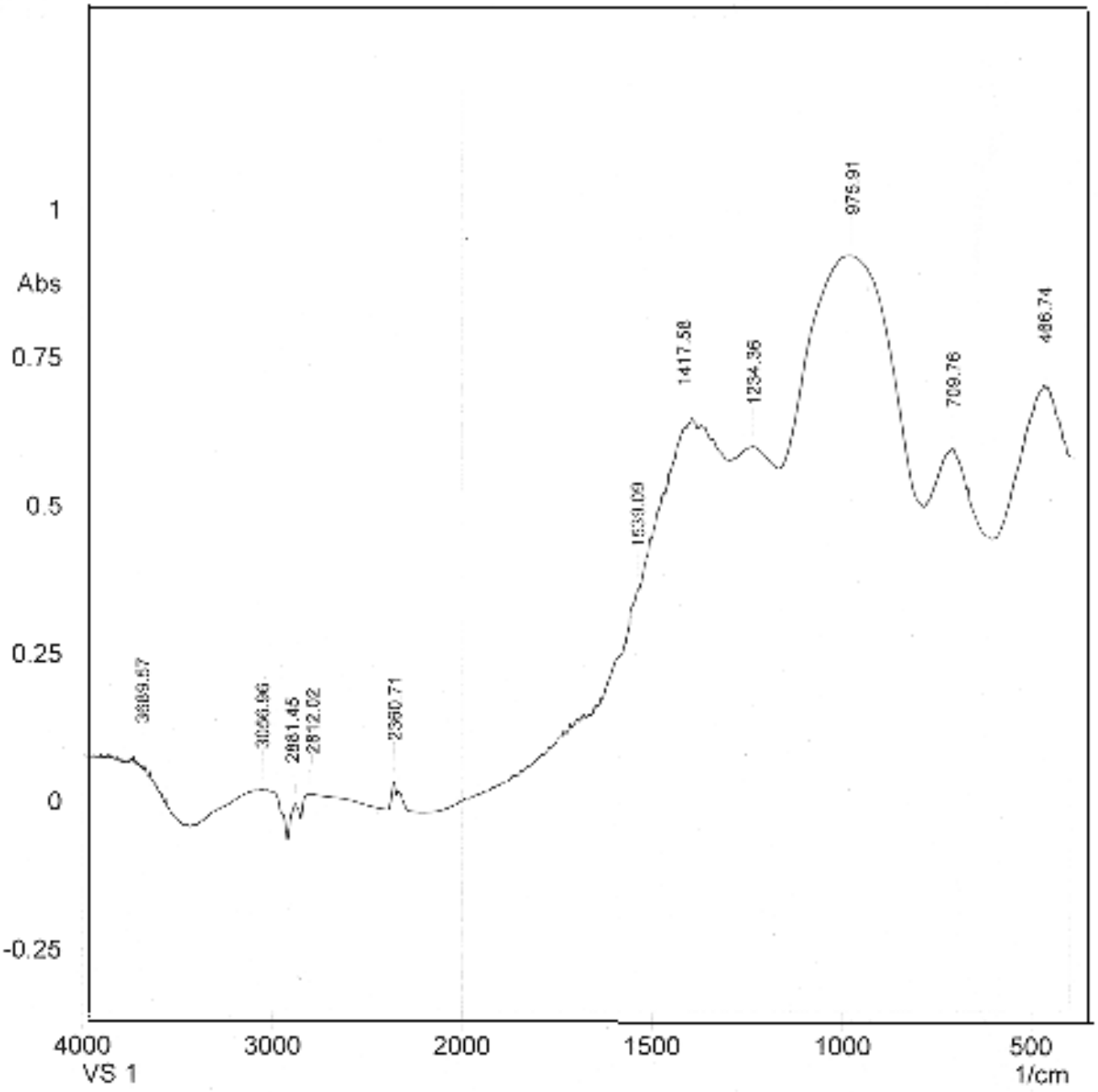

Fig. 6.19 FTIR spectra of sample VS1

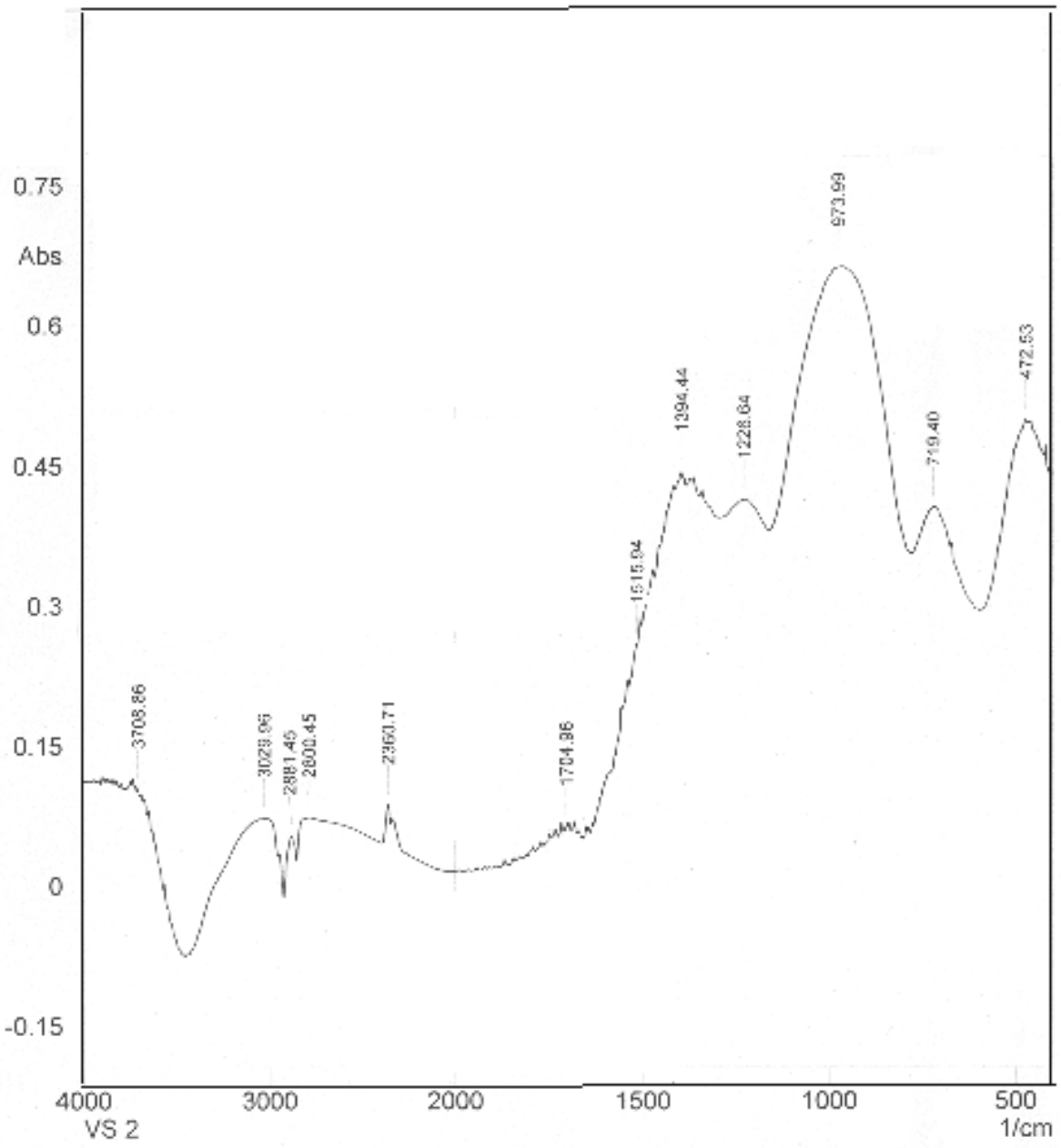

Fig. 6.20 FTIR spectra of sample VS2

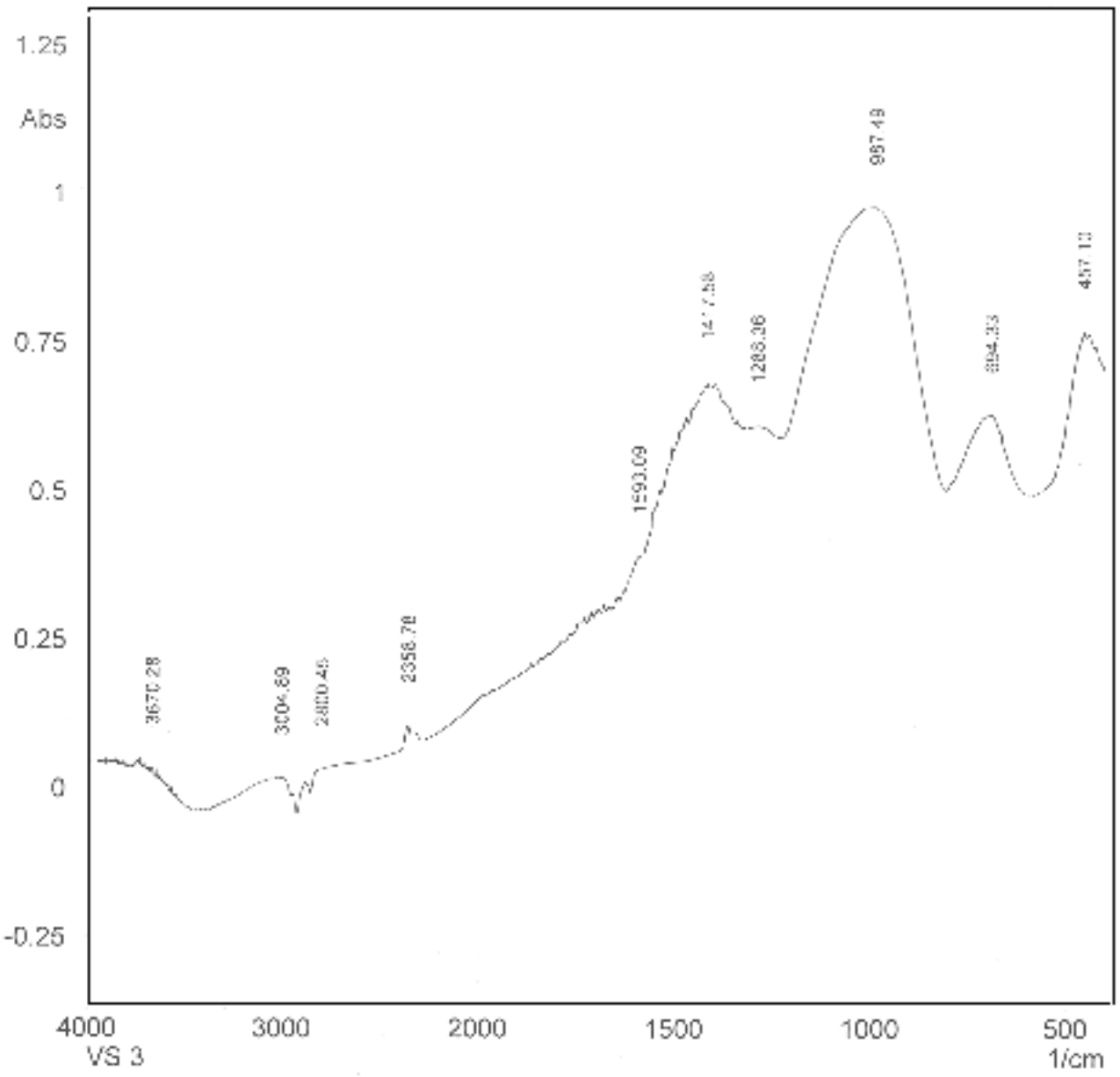

Fig. 6.21 FTIR spectra of sample VS 3

Table 5: Peak Assignment of the FTIR spectra

Wave number (cm^{-1})	Peak Assignment
462 - 472.53	Si-O-Si and O-Si-O bending modes
669.25	C-Br axial stretching
694.33	Atoms oxygen bridges between trigonal atoms (BO_4 stretching)
705.9 - 709.63	Atoms oxygen bridges between trigonal atoms(BO_4 stretching)
923.84	$Si-O^-$ Stretching with two non bridging oxygens
937.4 - 987.49	Diborate (BO_4 stretching)
1070.42, 1076.21	Si-O-Si anti-symmetric –stretching of bridging oxygen within the tetrahedral
1249 , 1234.36, 1226.64	Boroxol rings, tri, tetra and pentaborate groups pyro and other borates (BO_3 stretching)
1288.36	C-O stretching
1394.44, 1417.58 , 1419.51, 1515.94	B-O vibrations of various borate groups(BO_3stretching)
1548.73, 1539.09	B-O bonds vibration (BO_3 stretching)

Table 6: Showing values of T_s, TEC and FTIR peaks for all samples

Sample name	T_s(°C)	TEC(X 10^{-6}/°C)	FTIR Peak
VS1	650	7.76	BO_4 stretching
VS2	620	5.26	BO_4 stretching
VS3	_	_	BO_4 stretching
VM1	620	4.7	Si-O-Si antisymmetric stretching
VM2	730	3.03	BO_4 stretching
VM3	735	1.99	Si-O-Si antisymmetric stretching

Figures 6.16-6.21 show the absorption spectra for all the six samples. The spectra peaks are assigned using table 6. In case of FTIR spectra of samples having SrO the prominent peak in the spectra is due to the presence of BO_4 (borate stretching) where as in case of MgO based sample a prominent peak belongs to Si-O-Si antisymmetric stretching. It means the MgO based samples are dominated by Si-O tetrahedral bonding while SrO based samples show prominently BO_4 bonding. The softening temperature of these-glasse samples is also low as compared to MgO based glasses. This may be again explained on the basis of field strength as Si^{4+} exhibit higher field strength (1.38/ A^{o2}) than BO^{3+}(1.21/ A^{o2}).

CHAPTER 7

CONCLUSIONS & FUTURE ASPECT

7. Conclusions:

For most SOFC designs, the sealing material must have thermal expansion characteristics that do not contribute to the formation of thermal stresses between a variety of ceramic and metallic materials used in the SOFC stack; must be thermochemically compatible with those other materials; must remain stable at elevated temperatures (700-800°C) over the lifetime of the SOFC (thousands of hours), in the oxidizing and reducing environments of an SOFC cell.

The series of glass ceramic SiO_2-B_2O_3-MgO/SrO-AO (A=Y^{3+}, La^{3+} and Al^{3+}) were prepared and characterized by XRD, TGA, Dilatometerey and FTIR techniques. These glasses were heat treated to understand their crystallization kinetics for various heat treatment durations. VS3 sample exhibit the presence of celsian phase after 10 hours heat treatment. Crystalline phases present in sample VS2 could not be indexed with available PDF data. Apart from these two samples all other samples were amorphous after heat treatment at 800^oC for 1 hour and 10 hours.

The MgO based glass sealants prepared by La, Al, Y doping have shown higher crystallization temperatures as compared to SrO based glass samples which makes these sealants suitable for high temperature applications.

Commercialization efforts are focused on the links between the fuel cell design and the materials development is presumably linked closely with the designs. The global objective of the proposed research is to establish the fundamental materials behavior during the interaction of the sealing glass with metal interconnects

This may be attributed due to higher field strength of Mg^{2+} than Sr^{2+}. Thermal expansion of VS1 sample is higher than other samples and it is comparable to the other components of SOFC. VM3 sample is more stable than VS3 sample.

In the context of commercialization, this information will be used to guide additional materials development for sealing glasses and interconnect alloys, and for computer modeling that is used in designing cell

The interaction of the candidate sealing glasses with the candidate metallic interconnects has been studied in some detail, but much work remains to fully understand the underlying phase relations, reactivity, and kinetics.

Suggestions for Future Work:

In order to understand the stability of the present samples, it is essential to give heat treatment at higher temperature (say 950^{o}C) for longer duration (100 hours). Various phase formation and their reactivity with other components of SOFC also be studied after prolonged heat treatment to check their suitability as a sealing material.

REFERENCES:

[1] L. Carrette, K. A. Friedrich, U. Stimming, ChemPhysChem 1 (2000) 162.

[2] K. Scott Weil, John E. Deibter, John S Hardy, Dong Sang Kim, Guan-Guang Xia, L A Chick and Chris A Coyle, J. Mat. Eng. and Perf. 13 [3] (2003).

[3] K. L. Ley, M. Krumplet, R. Kumar, J. H. Meiser and I.J. Bloom, J. Mat. Res. 11 (1996) 1489.

[4] P. H. Larsen, F. W. Poulsen, R. W. Berg, J. Non-Cryst. Solid. 244 (1999) 16.

[5] N.Lahl, K. Singh, L. Singheiser, K. Hilpert, D. Bahadur, J. Mat. Sci. 35 (2000) 3089.

[6] N. Lahl, L. Singheiser, K. Hilpert, K. Singh, D. Bahadur, in: S. Singhal, M. Dokiya (Eds.), Solid Oxide Fuel Cells-VI, Electrochemical Society, Pennington, NJ, PV 99-19, 1999, p. 1057.

[7] N. Lahl, D. Bahadur, K. Singh, L. Singheiser, K. Hilpert, J. Electrochem. Soc. 149 (2002) A607.

[8] N. Q. Minh, J. Am. Ceram. Soc. 76 (1993) 563.

[9] K. Eichler, G. Solow, P. Otschik and W. Schaffrath, J. Eur. Ceram. Soc. 19 (1999) 1101.

[10] K. S. Weil, C. A. Coyle, J. S. Hardy, J. Y. Kim and G.-G. Xia, Fuel Cells Bull. May 2004, p. 11.

[11] P. H. Larsen and P. F. James, J. Mater. Sci. 33 (1998) 2499.

[12] R. W. Rice, in "Advances in Joining Technology" edited by J. J. Burke, A. E. Gorum, and A. Tarpinian, (Brook Hill Publishing, Chestnut Hill, MA 1976).

[13] M. G. Nicholas, "Joining Structural Ceramics" In Designing Interfaces for Technological Applications, edited by S. D. Peteves, (Elsevier Appl. Science, Amsterdam, 1989) p. 49.

[14] K. Suganuma, T. Okamoto, M. Shimada and M. Koizumi, J. Am. Ceram. Soc. 66 (1983) C117.

[15] M. Koizumi, T. Okamoto, M. Shimada, K. Suganuma, Am. Ceram. Soc. Bull. 63 (1984) 1173.

[16] K. Suganuma, T. Okamoto, M. Koizumi and M. Shimada, J. Am. Ceram. Soc. 67 (1984) C256.

[17] K. Suganuma, T. Okamoto, M. Koizumi, M. Shimada, J. Am. Ceram. Soc. 68 (1985) C334.

[18] K. Suganuma, T. Okamoto, Y. Miyamoto, M. Shimada and M. Koizumi, Mater. Sci. Tech. 2 (1986) 1156.

[19] K. Suganuma, T. Okamoto, M. Koizumi, M. Shimada, J. Mater. Sci. 22 (1987) 1359.

[20] W. G. Nicholas and D. A. Mortimer, Mater. Sci. Tech. 1 (1985) 657.

[21] W. A Owczarski, D. F Paulonis, Welding J. 62 (1981) 22.

[22] B. Alman, I. Guterrez, J. Urcola, Scripta Mater. 36 (1997) 509.

[23] D. R. Askeland, in "The science and engineer of materials" (Hong Kong: Nan Nostrand Reinhold; 1989).

[24] E. Pippel, J. Woltersdorf, P. Colombo and A. Donato, J. Eur. Ceram. Soc. 17 (1997) 1259.

[25] M. M. Schwartz, Brazing ASM International, Metals Park, Ohio p. 47

[26] C. W. Fox and G. M. Slaughter, Welding J. 43 (1964) 591.

[27] O. M. Akselsen, J. Mater. Sci. 27 (1992) 1989.

[28] J. P. Rice, D. M. Paxton and K. S. Weil, in Proceedings of 26th Annual Conference on Composites, Advanced Ceramics, Materials and Structures: B, edited by H.-T. Lin and M. Singh, (American Ceramic Society, Westerville, OH, USA, 2002).

[29] J. W. Stevenson, T. R. Armstrong, R. D. Carneim, L. R. Pederson and W. J. Weber, J. Electrochem. Soc. 143 (1996) 2722.

[30] J. S. Hardy, J. Y. Kim and K. S. Weil, J. Electrochem. Soc. 151 (2004) J43.

[31] Y.-S Chou, J. W. Stevenson and L. A. Chick, J. Power Sources 112 (2002) 130.

[32] S. P. Simner, J. W. Stevenson, J. Power Sources 102 (2001) 310.

[33] J. Kim, A. Virkar, in, "Solid Oxide Fuel Cells-VI" , edited by S. Singhal, M. Dokiya (Electrochemical Society, Pennington, NJ, PV 99-19, 1999) p. 830.

[34] Y.-S Chou and J. W. Stevenson, J. Power Sources 115 (2003) 274.

[35] Y.-S Chou and J. W. Stevenson, J. Power Sources 124 (2003) 473.

[36] Y.-S Chou and J. W. Stevenson, J. Power Sources 135 (2004) 72.

[37] Y.-S Chou and J. W. Stevenson, J. Power Sources 140 (2005) 340.

[38] M. Bram, S. Reckers, P. Drinovac, J. Mönch, R. W. Steinbrech, H. P. Buchkremer and D. Stöver, J. Power Sources 138 (2004) 111.

[39] Y.-S Chou, J. W. Stevenson, L. A. Chick, J. Am. Ceram. Soc. 86 (2003) 1003.

[40] Y.-S Chou and J. W. Stevenson, J. Power Sources 112 (2002) 376.

[41] D. Ghosh, S. Thompson, U. S. Pat, 6902798 (June7, 2005)

[42] K. Scott Weil, John E Deibler, John S Hardy, Dong Sang Kim, Guan Guang Xia, L A Chick and Chris A Coyle, J. Mat. Eng. Perf. 13[3] (2004) 316.

[43] G. Kirchoff, M. Holzherr, U. Bast and U. Rettig, Key Eng. Mater. 89-91 (1994) 605-10.

[44] G. Qian, T. Nakamura and C. C. Berndt, Mech. Mater. 27 (1998) 91-110.

[45] S.-B. Sohn, S.-Y. Choi, G.-H. Kim, H.-S. Song and G.-D. Kim, J. Am. Ceram. Soc., 87 [2] (2004) 254.

[46] S.-B. Sohn, S.-Y. Choi, G.-H. Kim, H.-S. Song and G.-D. Kim, J. Non-Cryst. Solids 297 (2002) 103.

[47] T. Schwickert, R. Sievering, P. Geasee and R. Conradt, Mat.-wiss.u. Werkstofftech. 33 (2002) 363.

[48] N. Lahl, L. Singheiser, K. Hilpert, K. Singh, D. Bahadur, in: S. Singhal, M. Dokiya (Eds.), Solid Oxide Fuel Cells-VI, Electrochemical Society, Pennington, NJ, PV 99-19, 1999, p. 1057.

[49] D. Bahadur, N. Lahl, K. Singh, L. Singheiser, K. Hilpert, D. Bahadur, J. Electrochem. Soc. 151 (2004) A558.

[50] C. Lara, M. J. Pauscal, A. Duran, J. Non-Cryst. Solid. 348 (2004) 149.

[51] Z. Yang, K. D. Meinhardt, J. W. Stevenson, Journal of Electrochemical Society, 150 (2003) A1095.

[52] Robert A Meyers, Encyclopedia of Physical Science and Technology Vol. 6, Academic Press Inc. 1987.

[53] S. P.Jiang, L. Christiansen, B. Hughan, K. Foger, J. Mat. Sci. Lett. 20 (2001) 695.

[54] N. Gupta, K. Singh, O. P. Pandey in: Proceedings of the National Conference on Materials and Related Technologies, September 19-20, 2003 pp. 141.

[55] C. Lara, M. J. Pauscal, M. O. Prado, A. Duran, Solid State Ionics 170 (2004) 201.

[56] C. Lara, M. J. Pauscal, A. Duran, Bol. Soc. Esp. Ceram. Vidr. 42 (2003) 133. [57]Z. Yang, X. Guangguang, K. D. Meinhardt, K. Scott Weil and J. W. Stevenson, J. Mat. Eng. and Perf. 13 (2004) 327.

[58] Z. Yang, J. W. Stevenson, K. D. Meinhardt, Solid State Ionics 160 (2003) 213.

[59] V. A. C. Haanappel, V. Shemet, I. C. Vinke, W. J. Quadakkers, J. Power Sources 141 (2005) 102.

[60] V. A. C. Haanappel, V. Shemet, I. C. Vinke, S. M. Gross, TH. Koppitz, N. H. Menzler, M. Zahid, W. J. Quadakkers, J. Mater. Sci. 40 (2005) 1583.

[61] V. A. C. Haanappel, V. Shemet, S. M. Gross, Th. Koppitz, N. H. Menzler, M. Zahid, W. J. Quadakkers, J. Power Sources xxx (2005) xxx (In Press)

[62] P. Batfalsky, V. A. C. Haanappel, J. Malzbender, N. H. Menzler, V. Shemet, I. C. Vinke, R. W. Steinbrech, J. Power Sources xxx (2005) xxx (In Press).

[63] N. P. Bansal and E. A. Gamble, J. Power Sources xxx (2005) xxx (In Press).

[64] P. Geasee, T. Schwickert, U. Diekmann, R. Conradt, in:J. G. Heinrich, F. Aldinger (EDS.), Ceramic Materials and components for engines, Wiley-VCH Verlag GmbH, Weinheim, Geramny, 57 (2001).

[65] T. Schwickert, U. Reisgen, P. Geasee, R. Conradt, J. Adv. Mater. 35 (2003) 44.

[66] K. Eichler, G. Solow, P. Otschik, W. Schaffrath, in: A.J. McEvoy(Ed.), European Solid Oxide Fuel Cell Forum Proceeedings, vol. 2, The European Fuel Cell Forum, Lucerne, Switzerland (2000), 899.

[67] F. Teitz, Ionics 5 (1999) 129.

[68] Yoshihiko Imanaka, Shigenori Akoi, Nobuo Kamehara and Koichi Niwa, J. Am. Cer. Soc. 78 (1995) 1265.